

# Unsupervised Point Cloud Representation Learning with Deep Neural Networks: A Survey

Aoran Xiao, Jiaying Huang, Dayan Guan, Xiaoqin Zhang, and Shijian Lu\*

**Abstract**—Point cloud data have been widely explored due to its superior accuracy and robustness under various adverse situations. Meanwhile, deep neural networks (DNNs) have achieved very impressive success in various applications such as surveillance and autonomous driving. The convergence of point cloud and DNNs has led to many deep point cloud models, largely trained under the supervision of large-scale and densely-labelled point cloud data. Unsupervised point cloud representation learning, which aims to learn general and useful point cloud representations from unlabelled point cloud data, has recently attracted increasing attention due to the constraint in large-scale point cloud labelling. This paper provides a comprehensive review of unsupervised point cloud representation learning using DNNs. It first describes the motivation, general pipelines as well as terminologies of the recent studies. Relevant background including widely adopted point cloud datasets and DNN architectures is then briefly presented. This is followed by an extensive discussion of existing unsupervised point cloud representation learning methods according to their technical approaches. We also quantitatively benchmark and discuss the reviewed methods over multiple widely adopted point cloud datasets. Finally, we share our humble opinion about several challenges and problems that could be pursued in the future research in unsupervised point cloud representation learning. A project associated with this survey has been built at [https://github.com/xiaoaraoan/3d\\_url\\_survey](https://github.com/xiaoaraoan/3d_url_survey).

**Index Terms**—Point Cloud, Unsupervised Representation Learning, Self-supervised Learning, Deep Learning, Transfer Learning.

## 1 INTRODUCTION

3D acquisition technologies have experienced fast development in recent years. This can be witnessed by different 3D sensors that have become increasingly popular in both industrial and our daily lives such as LiDAR sensors in autonomous vehicles, RGB-D cameras in Kinect and Apple devices, 3D scanners in various reconstruction tasks, etc. Meanwhile, 3D data of different modalities such as meshes, point clouds, depth images and volumetric grids, which capture accurate geometric information for both objects and scenes, have been collected and widely applied in different areas such as autonomous driving, robotics, medical treatment, remote sensing, etc.

Point cloud as one source of ubiquitous and widely used 3D data can be directly captured with entry-level depth sensors before triangulating into meshes or converting to voxels. This makes it easily applicable to various 3D scene understanding tasks [1] such as 3D object detection and shape analysis, semantic segmentation, etc. With the advance of deep neural networks (DNNs), point cloud understanding has attracted increasing attention as observed by a large number of deep architectures and deep models developed in recent years [2]. On the other hand, effective training of deep networks requires large-scale human-annotated training data such as 3D bounding boxes for object detection and point-wise annotations for semantic segmentation, which are usually laborious and time-consuming to collect due to 3D view changes and visual inconsistency between human

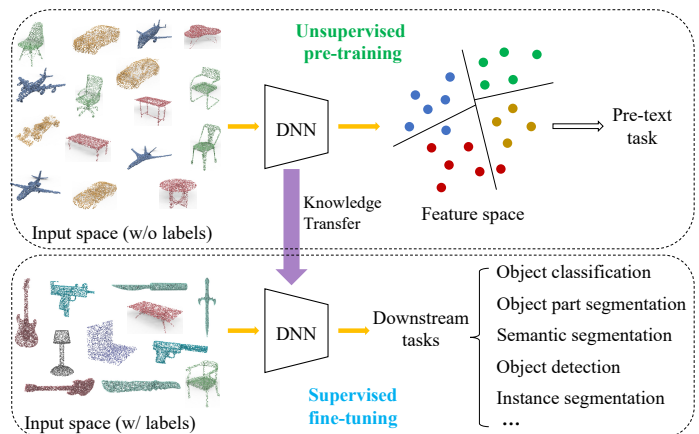


Fig. 1: The general pipeline of unsupervised representation learning on point clouds: Deep neural networks are first pre-trained with unannotated point clouds via unsupervised learning over certain pre-text tasks. The learned unsupervised point cloud representations are then transferred to various downstream tasks to provide network initialization, with which the pre-trained networks are *fine-tuned* with a small amount of annotated task-specific point cloud data.

perception and point cloud display. Efficient collection of large-scale annotated point clouds has become one bottleneck for effective design, evaluations, and deployment of deep networks while handling various real-world tasks [3].

Unsupervised representation learning (URL), which aims to learn robust and general feature representations from unlabelled data, has recently been studied intensively for mitigating the laborious and time-consuming data annotation challenge. As Fig. 1 shows, URL works in the

- Aoran Xiao, Jiaying Huang, Dayan Guan and Shijian Lu are with the School of Computer Science and Engineering, Nanyang Technological University, Singapore. E-mail: see <https://sg-vilab.github.io/people/>
- Xiaoqin Zhang is with Wenzhou University, China. Email: zhangxiaoqin-nan@gmail.com
- \*Corresponding author

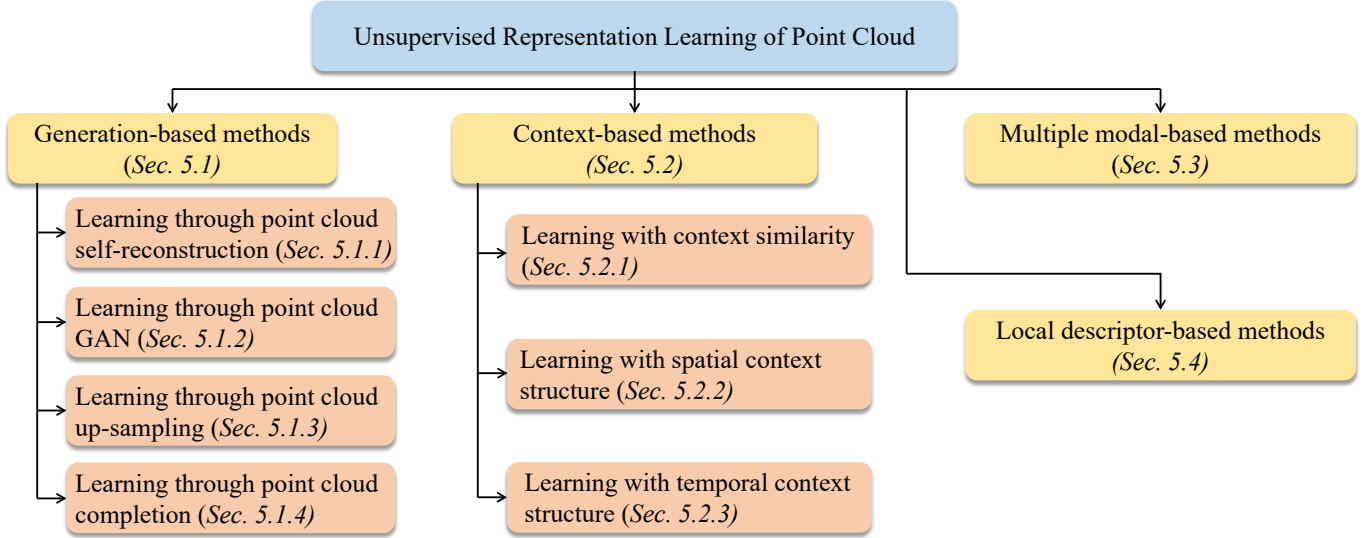


Fig. 2: Taxonomy of existing unsupervised methods in point cloud representation learning.

similar way to pre-training which learns useful knowledge from unlabelled data and transfers the learnt knowledge to various downstream tasks [4]. More specifically, URL can provide useful network initialization with which well-performing network models can be trained with a small amount of labelled and task-specific training data without suffering from much over-fitting as compared with training from random initialization. URL can thus help reduce training data and annotations which has demonstrated great effectiveness in the areas of natural language processing (NLP) [5], [6], 2D computer vision [7], [8], [9], [10], etc.

Similar to URL from other types of data such as texts and 2D images, URL of point clouds has recently attracted increasing attention in the computer vision research community. A number of URL techniques have been reported which are typically achieved by designing different pre-text tasks such as 3D object reconstruction [11], partial object completion [12], 3D jigsaws solving [13], etc. However, URL of point clouds still lags far behind as compared with its counterparts in NLP and 2D computer vision tasks. For the time being, training from scratch on various target new data is still the prevalent approach in most existing 3D scene understanding development. At the other end, URL from point cloud data is facing increasing problems and challenges, largely due to the lack of large-scale and high-quality point cloud data, unified deep backbone architectures, generalizable technical approaches, as well as comprehensive public benchmarks.

In addition, URL for point clouds is still short of systematic survey that can offer a clear big picture about this new yet challenging task. To fill up this gap, this paper presents a comprehensive survey on the recent progress in unsupervised point cloud representation learning from the perspective of datasets, network architectures, technical approaches, performance benchmarking, and future research directions. As shown in Fig. 2, we broadly group existing methods into four categories based on their technical approaches, including URL methods using data generation, global and local contexts, multimodality data and local descriptors,

more details to be discussed in the ensuing subsections.

The major contributions of this work can be summarized in three points as listed:

- 1) It presents a comprehensive review of the recent development in unsupervised point cloud representation learning. To the best of our knowledge, it is the *first* survey that provides an overview and big picture for this exciting research topic.
- 2) It studies the most recent progress of unsupervised point cloud representation learning, including a comprehensive benchmarking and discussion of existing methods over multiple public datasets.
- 3) It shares several research challenges and potential research directions that could be pursued in unsupervised point cloud representation learning.

The rest of this survey is organized as follows: In Section 2, we introduce background knowledge of unsupervised point cloud learning including term definition, common tasks of point cloud understanding and relevant surveys to this work. Section 3 introduces widely-used datasets and their characteristics. Section 4 introduces commonly used deep point cloud architectures with typical models that are frequently used for point cloud URL. In Section 5 we systematically review the methods for point cloud URL. Section 6 summarizes and compares the performances of existing methods on multiple benchmark datasets. At last, we list several promising future directions for unsupervised point cloud representation learning in Section 7.

## 2 BACKGROUND

### 2.1 Basic concepts

We first define all relevant terms and concepts that are to be used in the ensuing sections.

**Point cloud data:** A point cloud  $P$  is a set of vectors  $P = \{p_1, \dots, p_N\}$  where each vector represents one point  $p_i = [C_i, A_i]$ . Here,  $C_i \in \mathbf{R}^{1 \times 3}$  refers to 3D coordinate  $(x_i, y_i, z_i)$  of the point, and  $A_i$  refers to feature attributes of the point

such as RGB values, LiDAR intensity, normal values, etc., which are optional and variational depending on 3D sensors as well as applications.

**Supervised learning:** Under the paradigm of deep learning, supervised learning aims to train deep network models by using labelled training data.

**Unsupervised learning:** Opposite to supervised learning, unsupervised learning aims to train networks by using unlabelled training data.

**Unsupervised representation learning:** URL is a subset of unsupervised learning. It aims to learn meaningful representations from data without using any data labels/annotations, where the learnt representations can be transferred to different downstream tasks.

**Semi-supervised learning:** In semi-supervised learning, deep networks are trained with a small amount of labelled data and a large amount of unlabelled data. It aims to mitigate data annotation constraint by learning from a small amount of labelled data and a large amount of unlabelled data that have similar distributions.

**Pre-training:** Network pre-training aims for pre-trained models by training with certain pre-text tasks over other datasets. The learned parameters are often employed for model initialization for further fine-tuning with various task-specific data.

**Transfer learning:** Transfer learning aims to transfer knowledge across tasks, modalities or datasets. A typical scenario related to this survey is to perform unsupervised learning for pre-training for transferring the learnt knowledge from unlabelled data to various downstream networks.

## 2.2 Common 3D understanding tasks

This subsection introduces common 3D understanding tasks including *object-level tasks* in object classification and object part segmentation and *scene-level tasks* in 3D object detection, semantic segmentation and instance segmentation. These tasks have been widely adopted to evaluate the quality of point cloud representations that are learned via various unsupervised learning methods. Typically, the learned unsupervised representations are employed for network initialization for these down-stream tasks, where the performance of the fine-tuned task models shows the quality of the learnt unsupervised representations.

### 2.2.1 Object classification

Object classification aims to classify point cloud objects into a number of pre-defined categories. Two evaluation metrics are most frequently used: The *overall Accuracy* (OA) represents the averaged accuracy for all instances in the test set; The *mean class accuracy* (mAcc) represents the mean accuracy of all object classes for the test set.

In addition, two evaluation protocols have been widely adopted while using object classification as the downstream task for evaluating the quality of the learnt unsupervised representations. The first is the *linear classification protocol*: A linear SVM classifier is trained with the learnt unsupervised representations together with the labels of the training data and the accuracy of the linear classifier on the testing set is reported for evaluations and comparisons. It requires unsupervised learning methods to capture semantic structures

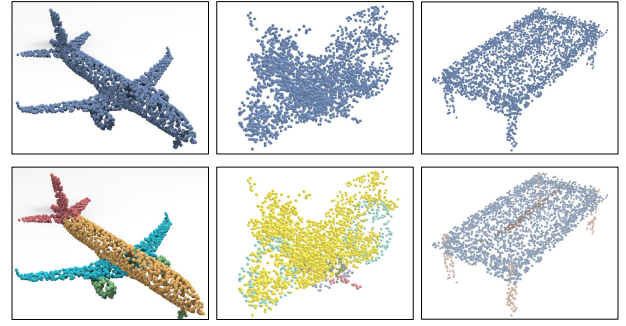


Fig. 3: Illustration of object part segmentation: The first row shows a few object samples including *airplane*, *motorcycle*, and *table* from the ShapeNetPart dataset [14]. The second row shows segmentation ground truth with different parts as highlighted by different colors.

from point clouds, *e. g.* objects of the same categories should be close in the feature space and vice versa. The second is the *fine-tuning protocol*: The learnt unsupervised representations are used to initialize object classification networks, and the performance of the fine-tuned object classification model is employed for evaluating the generalization capability of the learned unsupervised representations.

### 2.2.2 Object part segmentation

Object part segmentation is an important task for point cloud representation learning. It aims to assign a part category label (*e.g.*, airplane wing, table leg, etc.) to each point as illustrated in Fig. 3. The mean Intersection over Union (mIoU) [15] is the most widely adopted evaluation metric. For each instance, IoU is computed for each part belonging to that object category. The mean of the part IoUs represents the IoU of that object instance. The overall IoU is computed as the average of IoUs over all test instances while category-wise IoU (or class IoU) is calculated as the mean over instances under that category. Similar to object classification as described in Section 2.2.1, point-wise linear classification and fine-tuning have been widely adopted for evaluating the quality of the learnt unsupervised point cloud representations.

### 2.2.3 3D object detection

3D Object detection on point clouds is a crucial and indispensable task for many real-world applications, such as

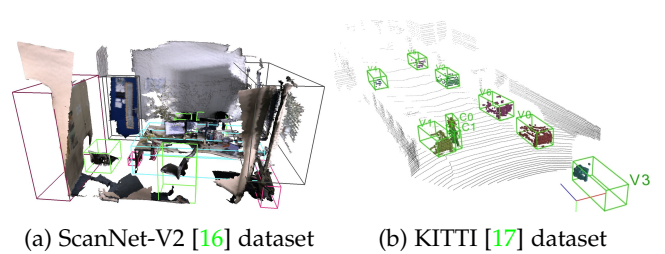


Fig. 4: Illustration of 3D bounding boxes in point cloud object detection: The two graphs show 3D bounding boxes in datasets ScanNet-V2 [16] and KITTI [17] which are cropped from [18] and [19], respectively.

autonomous driving and domestic robots. The task aims to localize objects in the 3D space, *i.e.* 3D object bounding boxes as illustrated in Fig. 4. The average precision (AP) metric has been widely used for evaluations in 3D object detection [18], [20]. While evaluating the learnt unsupervised representations, the pre-trained unsupervised model is fine-tuned over 3D object detection data for evaluating the generalization of the learned unsupervised representations.

#### 2.2.4 3D semantic segmentation

3D semantic segmentation on point clouds is another critical task for 3D understanding as illustrated in Fig. 5. Different from the object part segmentation that segments point cloud objects, 3D semantic segmentation aims to assign a category label to each point in scene-level point clouds. The widely adopted evaluation metrics includes OA, mIoU over semantic categories and mAcc. To assess the generalization capability of the learnt unsupervised representations, an unsupervised model is first pre-trained with certain pre-text tasks over large-scale unlabelled data. It is then fine-tuned over the training data of one specific 3D semantic segmentation dataset. The unsupervised representations can thus be evaluated by the segmentation performance of the fine-tuned model over the test data of the 3D dataset.

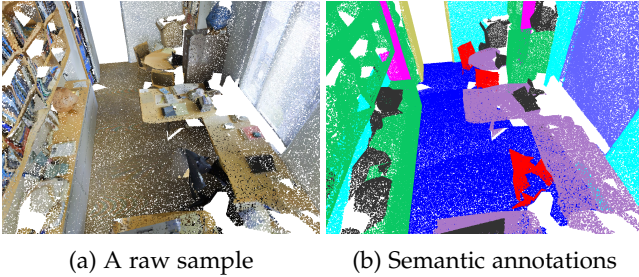


Fig. 5: Illustration of semantic point cloud segmentation: For the point cloud sample from S3DIS [21] on the left, the graph on the right shows the corresponding ground truth where different categories are highlighted by different colors.

#### 2.2.5 3D instance segmentation

3D instance segmentation aims to detect and delineate each distinct object of interest in scene-level point clouds as illustrated in Fig. 6. On top of semantic segmentation that considers the semantic category only, instance segmentation assigns each object with a unique identity. Mean Average Precision (mAP) has been widely adopted for quantitative evaluation of this task. Similar to the aforementioned tasks, networks initialized with the learnt unsupervised representations are fine-tuned on instance segmentation datasets, and the performance of the fine-tuned model over the test data is used to evaluate the generalization capability of the learnt unsupervised representations.

### 2.3 Relevant surveys

To the best of our knowledge, this paper is the *first* survey that reviews unsupervised point cloud learning comprehensively. Several relevant but different surveys have been performed. For example, several papers reviewed recent

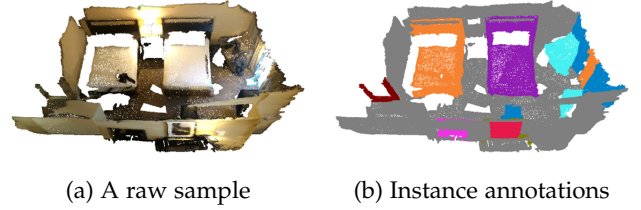


Fig. 6: Illustration of instance segmentation on point clouds: For the point cloud sample from ScanNet-V2 [16] on the left, the graph on the right shows the corresponding ground truth with different instances highlighted by different colors.

advances for deep supervised learning on point clouds: Anastasia *et al.* [22] reviewed deep learning approaches on 3D data; Xie *et al.* [23] provided a literature review on point cloud segmentation task; Guo *et al.* [2] provided a comprehensive and detailed survey on deep learning of point cloud for multiple tasks including classification, detection, tracking, and segmentation. In addition, several works reviewed unsupervised representation learning on other data modalities: Jing *et al.* [24] introduced advances on unsupervised representation learning in 2D computer vision; Liu *et al.* [25] looked into latest progress about unsupervised representation learning methods in 2D computer vision, NLP, and graph learning; Qi *et al.* [26] introduced recent progress on small data learning including unsupervised- and semi-supervised methods.

## 3 POINT CLOUD DATASETS

In this section, we summarize the commonly used datasets for training and evaluating unsupervised point cloud representation learning. Existing work learns unsupervised point cloud representations mainly from 1) synthetic object datasets including ModelNet [27] and ShapeNet [14], or 2) real scene datasets including ScanNet [16] and KITTI [17]. In addition, various tasks-specific datasets have been collected which can be used for fine-tuning downstream models, such as ScanObjectNN [29], ModelNet40 [27], and ShapeNet [14] for point cloud classification, ShapeNetPart [14] for part segmentation, S3DIS [21], ScanNet [16], or Synthia4D [31] for semantic segmentation, indoor datasets SUNRGB-D [28] and ScanNet [16] as well as outdoor dataset ONCE [30] for object detection.

- **ModelNet10/ModelNet40 [27]:** ModelNet is a synthetic object-level dataset for 3D classification. The original ModelNet provides CAD models represented by vertices and faces. Point clouds are generated by sampling from the models uniformly. ModelNet40 contains 13,834 objects of 40 categories, among which 9,843 objects forms the training set and the rest forms test set. ModelNet10 consists of 3,377 samples of 10 categories, which are split into 2,468 training samples and 909 testing samples.
- **ShapeNet [14]:** ShapeNet contains synthetic 3D objects of 55 categories. It was curated by collecting CAD models from online open-sourced 3D repositories. Similar to ModelNet, synthetic objects in

TABLE 1: Summary of commonly used datasets for training and evaluations in prior unsupervised point cloud representation learning research.

Dataset	Year	#Samples	#Classes	Type	Representation	Label
KITTI [17]	2013	15K frames	8	Outdoor driving	RGB & LiDAR	Bounding box
ModelNet10 [27]	2015	4,899 objects	10	Synthetic object	Mesh	Object category label
ModelNet40 [27]	2015	12,311 objects	40	Synthetic object	Mesh	Object category label
ShapeNet [14]	2015	51,190 objects	55	Synthetic object	Mesh	Object/part category label
SUN RGB-D [28]	2015	5K frames	37	Indoor scene	RGB-D	Bounding box
S3DIS [21]	2016	272 scans	13	Indoor scene	RGB-D	Point category label
ScanNet [16]	2017	1,513 scans	20	Indoor scene	RGB-D & mesh	Point category label & Bounding box
ScanObjectNN [29]	2019	2,902 objects	15	Real-world object	Points	Object category label
ONCE [30]	2021	1M scenes	5	Outdoor driving	RGB & LiDAR	Bounding box

ShapeNet are complete, aligned, and with no occlusion or background. Its extension **ShapeNetPart** has 16,881 objects of 16 categories and is represented by point clouds. Each object consists of 2 to 6 parts, and in total there are 50 part categories in the dataset.

- **ScanObjectNN [29]**: ScanObjectNN is a real object-level dataset, where 2,902 3D point cloud objects of 15 categories are constructed from the scans captured in real indoor scenes. Different from synthetic object datasets, point cloud objects in ScanObjectNN are noisy (including background points, occlusions, holes in objects) and not axis-aligned.
- **S3DIS [21]**: Stanford Large-Scale 3D Indoor Spaces (S3DIS) dataset contains over 215 million points scanned from 6 large-scale indoor areas in 3 office buildings, where each area is 6,000 square meters. The scans are represented as point clouds with point-wise semantic labels of 13 object categories.
- **ScanNet-V2 [16]**: ScanNet-V2 is a RGB-D video dataset containing 2.5 million views in more than 1500 scans, which are captured in indoor scenes such as offices and living rooms and annotated with 3D camera poses, surface reconstructions, as well as semantic and instance labels for segmentation.
- **SUN RGB-D [28]**: SUN RGB-D dataset is a collection of single view RGB-D images collected from indoor environments. There are in total 10,335 RGB-D images annotated with amodal, and 3D oriented object bounding boxes of 37 categories. KITTI is a pioneer outdoor dataset providing dense point clouds from a LiDAR sensor together with other modalities including front-facing stereo images and GPS/IMU data. It provides 200k 3D boxes over 22 scenes for 3D object detection.
- **ONCE [30]**: ONCE dataset has 1 million LiDAR scenes and 7 million corresponding camera images. There are 581 sequences in total, where 560 sequences are unlabelled and used for unsupervised learning, and 10 sequences are annotated and used for testing. It provides an unsupervised learning benchmark for object detection in outdoor environments.

The publicly available datasets for URL of point clouds are still limited in both data size and scene variety, especially compared with the image and text datasets that have been used for 2D computer vision and NLP research. For example, there are 800 million words in BooksCorpus and 2,500 million words in English Wikipedia that is able to provide comprehensive data sources for unsupervised representa-

tion learning in NLP [32]; ImageNet [33] has more than 10 million images for unsupervised visual representation learning. Large-scale and high-quality point cloud data are highly demanded for the future research on this topic, and we provide detailed discussion of this issue in Section 7.

#### 4 COMMON DEEP ARCHITECTURES

Over the last decade, deep learning approaches have been playing more important role in the processing and understanding of point cloud data. This can be observed by the abundance of new deep architectures that have been developed in recent years. Different from traditional 3D vision algorithms that transform point clouds to structures like Octrees [34] or Hashed Voxel Lists [35], deep learning approaches favor more amenable structures for differentiability and/or efficient neural processing which have achieved very impressive performance over various 3D tasks.

At the other end, DNN-based point cloud processing and understanding lags far behind as compared with its counterparts in NLP and 2D computer vision. This is especially true for the task of unsupervised representation learning, largely due to the lack of regular representations in point cloud data. Specifically, word embeddings and 2D images have regular and well-defined structures, but point clouds represented by unordered point sets have no such universal and structural data format.

In this section, we introduce deep architectures that have been explored for the URL of point cloud data. Deep learning for point clouds achieved significant progress during the last decade and we see the abundance of 3D deep architectures and 3D models being proposed. However, we do not have universal and ubiquitous “3D backbones” like VGG [36] or ResNet [37] in 2D computer vision. We therefore focus on those frequently used deep architectures in the URL of point clouds in this survey. For the clarity of description, we group them into five categories broadly, namely, point-based architectures, graph-based architectures, sparse voxel-based architectures, spatial CNN-based architectures, and Transformer-based architectures. Note other deep architectures have also been reported for various 3D tasks as discussed in [2], such as projection-based networks [38], [39], recurrent neural networks [40], 3D capsule networks [41], etc. However, they were not often employed for the URL task and thus are not detailed in this survey.

##### 4.1 Point-based deep architectures

Point-based networks [15], [42], [43], [44] were designed to process raw point cloud directly without point data



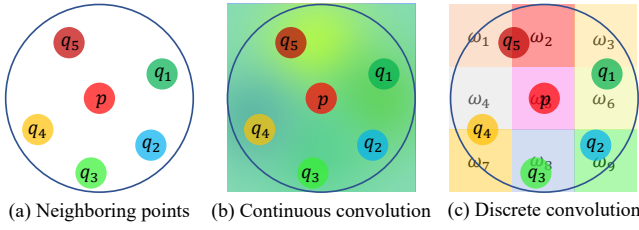


Fig. 10: An illustration of 3D spatial convolution including continuous and discrete convolutions. Parameters  $p$  and  $q_i$  denote the center point and its neighboring points, respectively. The graph is reproduced based on [2].

relations among local centers with their surrounding points, and it learns dynamic weights for convolutions.

#### 4.5 Transformer-based deep architectures

Over the last few years, Transformers have made astounding progress in the research areas of NLP [32], [52] and 2D image processing [53], [54] due to their structural superiority and versatility. They have also been introduced into the area of point cloud processing [55], [56] recently. Fig. 11 shows a standard Transformer architecture for URL of point clouds [56], which contains a stack of Transformer blocks [52] and each block consists of a multi-head self-attention layer and a feed-forward network. The unsupervised pre-trained Transformer encoder can be used for fine-tuning downstream tasks such as object classification and semantic segmentation, etc.

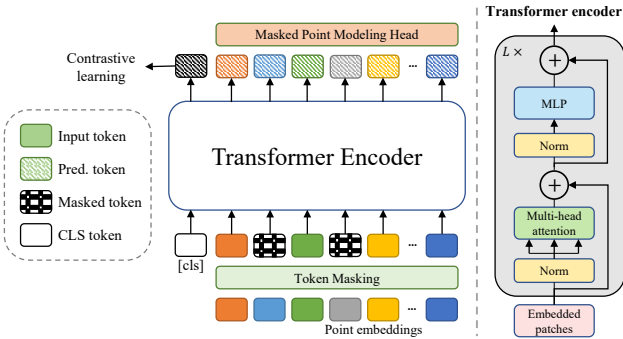


Fig. 11: The architecture of point cloud Transformer that was used for unsupervised pre-training in Point-BERT [56]. More network details can be found in [56]. The figure is reproduced based on [53], [56].

## 5 UNSUPERVISED POINT CLOUD REPRESENTATION LEARNING

In this section, we review existing URL methods for point clouds. As shown in Fig. 2, we broadly group existing methods into four categories according to their technical approaches, including generative-based methods, context-based methods, multiple modal-based methods, and local descriptor-based methods. With this taxonomy, we sort out existing methods and systematically introduce them in the ensuing subsections of this section.

### 5.1 Generation-based methods

Generation-based URL methods for point clouds involve the process of generating point cloud objects in training. According to the employed pre-text tasks, they can be further grouped into four subcategories including point cloud self-reconstruction (for generating point cloud objects that are the same as the input), point cloud GAN (for generating fake point cloud objects), point cloud up-sampling (for generating objects with denser point clouds but similar shapes) and point cloud completion (for predicting missing parts from incomplete point cloud objects). The ground truth of these URL methods are point clouds themselves. Hence, these methods require no human annotations and can learn in an unsupervised manner. Table 2 shows a list of generation-based methods.

#### 5.1.1 Learning through point cloud self-reconstruction

Networks for self-reconstruction usually encode point cloud samples into representation vectors and decode them back to the original input data, where shape information and semantic structures are extracted during this. It belongs to one typical URL approach since it does not involve any human annotations. One representative network is Autoencoder [74] that has an encoder network and a decoder network as illustrated in Fig. 12. The encoder compresses and encodes a point cloud object into a low-dimensional embedding vector (i.e., *codeword*) [61], which is then decoded back to the 3D space by the decoder.

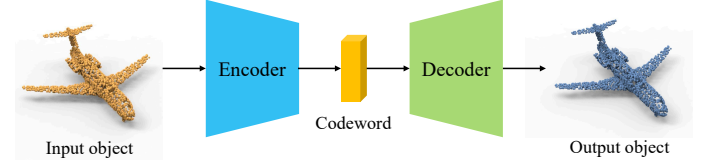


Fig. 12: An illustration of AutoEncoder in unsupervised point cloud representation learning: The *Encoder* learns to represent a point cloud object by a *Codeword* vector while the *Decoder* reconstructs the *Output Object* from the *Codeword*.

The model is optimized by forcing the final output to be the same as the input. During this process, the encoding is validated and learns by attempting to regenerate the input from the encoding whereas the autoencoder learns low-dimension representations by training the network to ignore insignificant data (“noise”) [75]. Permutation invariant losses [76] are widely adopted as the training objective to describe how the input and output point cloud objects are similar to each other. They can be measured by Chamfer Distance  $L_{CD}$  or Earth Mover’s Distance  $L_{EMD}$  as follows:

$$L_{CD} = \sum_{p \in P} \min_{p' \in P'} \|p - p'\| + \sum_{p' \in P'} \min_{p \in P} \|p' - p\| \quad (1)$$

$$L_{EMD} = \min_{\phi: P \rightarrow P'} \sum_{x \in P} \|p - \phi(p)\|_2 \quad (2)$$

Where  $P$  and  $P'$  denote input and output point clouds of the same size,  $\phi: P \rightarrow P'$  is bijection, and  $p$  &  $p'$  are points.

Self-reconstruction has been one of the most widely adopted pre-text tasks for URL from point clouds over the

TABLE 2: Summary of generation-based methods for unsupervised representation learning of point clouds.

Method	Publication	Year	Category	Contribution
VConv-DAE [57]	ECCV	2016	Completion	Learning by predicting missing parts in 3D grids
TL-Net [58]	ECCV	2016	Reconstruction	Learning by 3D generation and 2D prediction
3D-GAN [59]	NeurIPS	2016	GAN	Pioneer GAN for 3D voxels
3D-DescriptorNet [60]	CVPR	2018	Completion	learning with energy-based models
FoldingNet [61]	CVPR	2018	Reconstruction	learning by folding 3D object surfaces
SO-Net [62]	CVPR	2018	Reconstruction	Performing hierarchical feature extraction on individual points and SOM nodes
Latent-GAN [63]	ICML	2018	GAN	Pioneer GAN for raw point clouds and latent embeddings
MRT [64]	ECCV	2018	Reconstruction	A new autoencoder with multi-grid architecture
VIP-GAN [65]	AAAI	2019	GAN	Learning by solving multiple view inter-prediction tasks for objects with an RNN-based network
G-GAN [11]	ICLR	2019	GAN	Pioneer GAN with graph convolution
3DCapsuleNet [41]	CVPR	2019	Reconstruction	Learning with 3D point-capsule network
L2G-AE [66]	ACM MM	2019	Reconstruction	Learning by global and local reconstruction
MAP-VAE [67]	ICCV	2019	Reconstruction	Learning by reconstruction and half-to-half prediction
PointFlow [68]	ICCV	2019	Reconstruction	Learning by modeling point clouds as a distribution of distributions
PDL [69]	CVPR	2020	reconstruction	A probabilistic framework for point distribution learning
GraphTER [70]	CVPR	2020	Reconstruction	Proposed a graph-based autoencoder
SA-Net [71]	CVPR	2020	Completion	Learning by completing point cloud objects with a skip-attention mechanism
PointGrow [72]	WACV	2020	Reconstruction	Presented an autoregressive model that can recurrently generate point cloud samples.
PSG-Net [73]	ICCV	2021	Reconstruction	Learning by reconstruct point cloud objects with seed generation
OcCo [12]	ICCV	2021	Completion	Learning by completing occluded point cloud objects
Point-Bert [56]	CVPR	2022	Completion	Learning for Transformers by recovering masked object parts.

last decade. By assuming that point cloud representations should be generative in 3D space and predictable from 2D space, Girdhar *et al.* proposed TL-Net [58] that employs a 3D autoencoder to reconstruct 3D volumetric grids and a 2D convolutional network to learn 2D features from the projected images. Yang *et al.* designed FoldingNet [61] that introduces a folding-based decoder that deforms a canonical 2D grid onto the underlying 3D object surface of a point cloud object. Li *et al.* proposed SO-Net [62] that introduces self-organizing map to learn hierarchical features of point clouds via self-reconstruction. Zhao *et al.* [41] extended the capsule network [77] into 3D point cloud processing and the designed 3D capsule network can learn generic representations from unstructured 3D data. Gao *et al.* [70] proposed a graph-based autoencoder that can learn intrinsic patterns of point-cloud structures under both global and local transformations. Chen *et al.* [78] designed a deep autoencoder that exploits graph topology inference and filtering for extracting compact representations from 3D point clouds.

Several studies explore global and local geometries to learn robust representations from point cloud objects [66], [67]. For example, [66] introduces hierarchical self-attention in the encoder for information aggregation, and a recurrent neural network (RNN) as the decoder for point cloud reconstruction locally and globally. [67] presents MAP-VAE that introduces a half-to-half prediction task that first splits a point cloud object into a front half and a back half and then trains a RNN to predict the back half sequence from the corresponding front half sequence. Several studies instead formulate point cloud reconstruction as a point distribution leaning task [68], [69], [72]. For example, [68] presents PointFlow that generates 3D point clouds by modelling the distribution of shapes and that of points given shapes. [69] presents a probabilistic framework that extracts unsupervised shape descriptors via point distribution learning, which associates each point with a Gaussian and models point clouds as the distribution of points. [72] presents

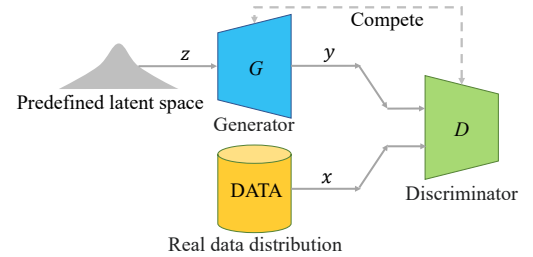


Fig. 13: An illustration of GAN which typically consists of a generator  $G$  and a discriminator  $D$  that fight with each other during the training process (in the form of a zero-sum game, where one agent's gain is another agent's loss).

an autoregressive model Pointgrow that generates diverse and realistic point cloud samples either from scratch or conditioned on semantic contexts.

Further, several studies learn point cloud representations from different object resolutions [64], [73], [79]. For example, Gadelha *et al.* [64] designed an autoencoder with a multi-resolution tree structure that learns point cloud representations via coarse-to-fine analysis. Yang *et al.* [73] proposed an autoencoder with a seed generation module that allows to extract input-dependent point-wise features in multiple stages with gradually increasing resolution. Chen *et al.* [79] proposed to learn sampling-invariant features by reconstructing point cloud objects of different resolution and minimizing Chamfer distances between them.

### 5.1.2 Learning through point cloud GAN

Generative and Adversarial Network (GAN) [80] is a typical deep generative network. As demonstrated in Fig. 13, it consists of a generator and a discriminator. The generator aims to synthesize as realistic data samples as possible while the discriminator tries to differentiate real samples and synthesized samples. GAN thus learns to generate new

data with the same statistics as the training set and the modeling can be formulated as a minmax problem:

$$\min_G \max_D L_{GAN} = \log D(x) + \log(1 - D(G(z))), \quad (3)$$

where  $G$  is the generator and  $D$  represents the discriminator.  $x$  and  $z$  represent a real sample and a randomly sampled noise vector from a distribution  $p(z)$ , respectively.

When training GANs for URL of point clouds, the generator learns from either a sampled vector or a latent embedding to generate point cloud instances, while the discriminator tries to distinguish whether input point clouds are from real data distribution or generated data distribution. The two sub-networks fight with each other during the training process and the discriminator learns to extract useful feature representations for point cloud object recognition. The learning process involves no human annotations thus the networks can be trained in an unsupervised learning manner. After that, the learned discriminator is extended into various downstream tasks such as object classification or part segmentation by fine-tuning the model.

Several networks employ GAN for URL for point clouds successfully [11], [59], [63], [81]. For example, Wu *et al.* [59] proposed the first GAN model applying for 3D voxels. However, the voxelization process either sacrifices the representation accuracy or incurs huge redundancies. Achlioptas *et al.* proposed Latent-GAN [63] as the first GAN model for raw point clouds. Li *et al.* [81] further proposed a point cloud GAN model with a hierarchical sampling and inference network that learns a stochastic procedure to generate new point cloud objects. Valsesia *et al.* [11] designed the first graph-based GAN model to extract localized features from point clouds. These methods evaluated the generalization of the learned representations by fine-tuning them to the high-level downstream 3D tasks.

### 5.1.3 Learning through point cloud up-sampling

As shown in Fig. 14, given a set of points, point cloud up-sampling aims to generate a denser set of points with similar geometries. This task requires deep point cloud networks to learn underlying geometries of 3D shapes without any supervision, and the learned representations can be used for fine-tuning in 3D downstream tasks.

Li *et al.* [82] introduced GAN into the point cloud up-sampling task and presented PU-GAN to learn a variety of point distributions from the latent space by up-sampling points over patches on object surfaces. The generator aims to produce up-sampled point clouds while the discriminator tries to distinguish whether its input point cloud is produced

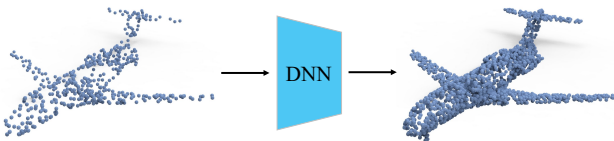


Fig. 14: An illustration of point cloud up-sampling: The network  $DNN$  learns point cloud representations by solving a pre-text task that reproduces an object with the same geometry but denser point distribution.

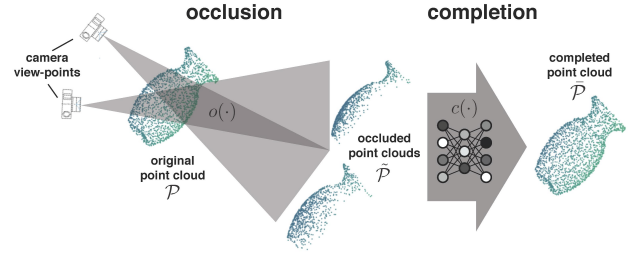


Fig. 15: The pipeline of OcCo [12]. Taking occluded point cloud objects as input, an encoder-decoder model is trained to complete the occluded point clouds, where the encoder learns point cloud representations and the decoder learns to generate complete objects. The learned encoder weights can be used for network initialization for downstream tasks. The figure is from [12] with author's permission.

by the generator or the real one. Similar to GANs introduced in Section 5.1.2, the learned discriminator can be transferred in downstream tasks. Remelli *et al.* [83] designed an autoencoder that can up-sample sparse point clouds into dense representations. The learned weight of the encoder can also be used as initialization weights for downstream tasks as described in Section 5.1.1. Though point cloud up-sampling is attracting increasing attention in recent years [82], [84], [85], [86], [87], [88], it is largely evaluated by the quality of generated point clouds while its performance in transfer learning has not been well studied.

### 5.1.4 Learning through point cloud completion

Point cloud completion is a task to predict arbitrary missing parts based on the rest of the 3D point clouds. To achieve this target, deep networks need to learn inner geometric structures and semantic knowledge of the 3D objects so as to correctly predict missing parts. On top of that, the learned representations can be transferred to downstream tasks. The whole process involves no human annotations and thus belongs to unsupervised representation learning.

Point cloud completion has been an active research area of 3D computer vision over the past decade [71], [99], [100], [101], [102], [103], [104] and learned feature representations have been evaluated in different unsupervised learning benchmarks [12], [57], [60], [71]. A pioneer work VConvDAE [57] voxelizes point cloud objects into volumetric grids and learns the shape distributions of 3D objects with an autoencoder that predicts the missing voxels from the rest parts. Xie *et al.* [60] presented a deep framework named 3D-DescriptorNet for probabilistic modeling of volumetric shape patterns. Achlioptas *et al.* [63] introduced the first DNN for raw point cloud completion which is a point-based network with an encoder-decoder structure. Yuan *et al.* [100] proposed the Point Completion Network (PCN) which is an autoencoder structured network, aiming to learn useful representations by repairing incomplete point cloud objects. Wen *et al.* [71] proposed another autoencoder for point cloud completion, namely SA-Net, which introduces a skip-attention mechanism in the encoder that selectively transfers geometric information from the local regions to the decoder for generating complete point cloud objects. Wang

TABLE 3: Summary of context-based methods for unsupervised representation learning of point clouds.

Method	Publication	Year	Category	Contribution
MultiTask [89]	ICCV	2019	Hybrid	Learning by clustering, reconstruction, and self-supervised classification
Jigsaw3D [13]	NeurIPS	2019	Spatial-context	Learning by solving 3D jigsaws
Contrast&Cluster [90]	3DV	2019	Hybrid	Learning by contrasting and clustering with GNN
GLR [91]	CVPR	2020	Hybrid	Learning by global-local reasoning
Info3D [92]	ECCV	2020	Context-similarity	Learning by contrasting global and local parts of objects
PointContrast [48]	ECCV	2020	Context-similarity	Learning by contrasting different views of scene point clouds
ACD [93]	ECCV	2020	Context-similarity	Learning by contrasting decomposed convex components
Rotation3D [94]	3DV	2020	Spatial-context	Learning by predicting rotation angle
HNS [95]	ACM MM	2021	Context-similarity	Learning by contrasting local patches of point cloud objects with hard negative sampling
CSC [3]	CVPR	2021	Context-similarity	Techniques to improve contrasting scene point cloud views
STRL [1]	ICCV	2021	Temporal-context	Learning spatio-temporal data invariance from point cloud sequences
RandomRooms [96]	ICCV	2021	Context-similarity	Constructing pseudo scenes with synthetic objects for contrastive learning
DepthContrast [97]	ICCV	2021	Context-similarity	Joint contrastive learning with points and voxels
SelfCorrection [98]	ICCV	2021	Hybrid	Learning by distinguishing and restoring destroyed objects

*et al.* [12] proposed to learn an encoder-decoder model that recovers the occluded points by different camera views as shown in Fig. 15. The encoder parameters are then used as initialization for downstream tasks including classification, part segmentation and semantic segmentation.

Recently, recovering missing parts from *masked* input as the pre-text task of URL has been proved remarkably successful in NLP [5], [6] and 2D computer vision [10]. Such idea has also been investigated in 3D point cloud learning [56], [105], [106], [107]. For example, Yu *et al.* [56] proposed a Point-BERT paradigm that pre-trains point cloud Transformers through a masked point modeling task. They use a discrete variational autoencoder to generate tokens for object patches and randomly masked out the tokens to train the Transformer to recover the original complete point tokens. The representations learned by Point-BERT can be well transferred to new tasks and domains such as object classification and object part segmentation.

### 5.1.5 Summary and discussion

Learning feature representations through different generation tasks is a major research direction for URL of point clouds. As described, different approaches have been proposed to learn representations from synthetic point cloud objects, *i.e.*, ModelNet and ShapeNet datasets. However, generating point clouds for indoor and outdoor scenes is a much more challenging task due to the large point numbers, heavy occlusion, complicated scene structures, etc. Therefore, few works explored learning 3D representations from generated scene-level data that have richer data distribution and wider potential applications. On the other hand, generation-based methods for URL have shown great successes in both NLP [6], [32] and 2D vision [10]. We expect more studies in this promising research direction.

## 5.2 Context-based methods

Context-based methods are another important category of URL of point clouds that has attracted increasing attention in recent years. Different from generation-based methods that learn representations in a generative way, these methods employ discriminative pre-text tasks to learn different context of point clouds including context similarity, spatial context structures, and temporal context structures. The

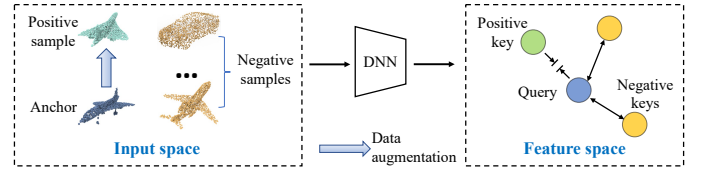


Fig. 16: An illustration of instance contrastive learning that learns locally smooth representations by self-discrimination, which pulls *Query* (from the *Anchor* sample) close to *Positive Key* (from *Positive Samples*) and pushes it away from *Negative Keys* (from *Negative Samples*).

designed pre-text tasks require no human annotations and Table 3 lists the recent methods.

### 5.2.1 Learning with context similarity

This type of method learns unsupervised representation of point clouds by exploring underlying context similarities between samples. A typical approach is *contrastive learning*, which has demonstrated superior performances in both 2D vision [7], [8], [108] and 3D vision [3], [48], [97] in recent years. Fig. 16 provides an illustration of the instance-wise contrastive learning. Given one input point cloud object instance as the anchor, its augmented views are defined as the positive samples while other different instances are negative samples. The network learns representations of point clouds by optimizing an self-discrimination task, *i.e.* query (feature of the anchor) should be close to the positive keys (features of positive samples) and faraway from its negative keys (features of negative samples). This learning strategy groups representations of similar samples together in an unsupervised manner and helps networks to learn semantic structures from unlabelled data distribution. The InfoNCE loss [109] defined below and its variants are often employed as the objective function in training:

$$\mathcal{L}_{\text{InfoNCE}} = -\log \frac{\exp(q \cdot k_+ / \tau)}{\sum_{i=0}^K \exp(q \cdot k_i / \tau)}, \quad (4)$$

where  $q$  is encoded query,  $\{k_0, k_1, k_2, \dots\}$  are keys with  $k_+$  being the positive key,  $\tau$  is a temperature hyper-parameter that controls how the distribution concentrates.

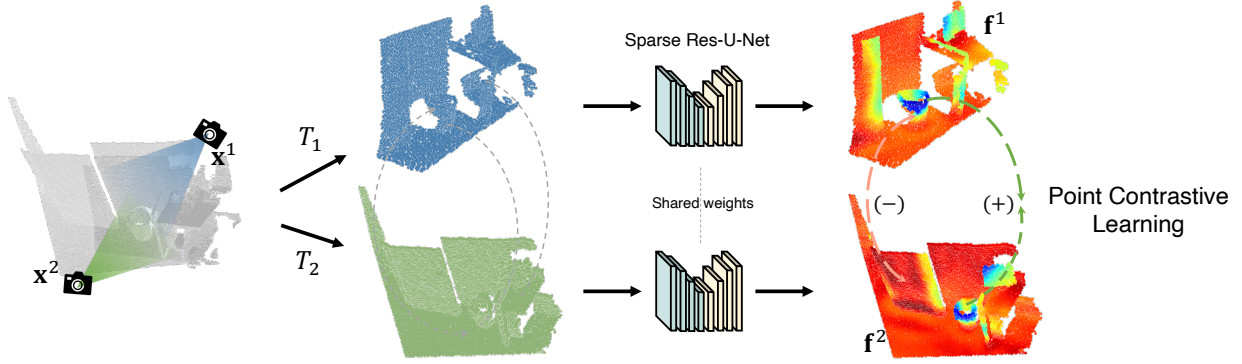


Fig. 17: The pipeline of PointContrast [48]: Two scans  $x^1$  and  $x^2$  of the same scene captured from two different viewpoints are transformed by  $T_1$  and  $T_2$  for data augmentation. The correspondence mapping between the two views is computed to minimize the distance for matched point features and maximize the distance for unmatched point features for contrastive learning. The graph is extracted from [48] with authors' permission.

Similar to generation-based methods, different contrastive learning methods [92], [93], [95], [110], [111] have been proposed to learn representations on *synthetic single objects*. For example, Sanghi *et al.* [92] proposed to learn useful feature representations by maximizing mutual information between synthetic objects and their local parts. Wang *et al.* [110] proposed a hybrid contrastive learning strategy that uses objects of different resolutions for instance-level contrast for capturing hierarchical global representations and simultaneously contrasted points and instances for learning local features. Gadelha *et al.* [93] decompose 3D objects into convex components and construct positive pairs among the same components and negative pairs among different components for the contrastive learning. Du *et al.* [95] introduced a hard negative sampling strategy into the contrastive learning between instances and local parts. Besides, Rao *et al.* [91] unified contrastive learning, normal estimation, and self-reconstruction into the same framework and formulated a multi-task learning method.

Recently, Xie *et al.* proposed PointContrast [48], a contrastive learning framework that learns representations of *scene* point clouds as illustrated in Fig. 17. The work shows, for the first time, that network weights pre-trained on 3D scene partial frames can lead to performance boosts when fine-tuned on multiple 3D high-level tasks including object classification, semantic segmentation, and object detection. Firstly, dense correspondences are extracted between two aligned views of ScanNet [16] to build point-pairs and point-level contrastive learning is then conducted with a unified backbone (SR-UNet). Finally, the learnt model was transferred to multiple downstream 3D tasks including classification, semantic segmentation, and object detection with consistent performance gains.

Since PointContrast brought new insights that the unsupervised representation learned from scene-level point clouds can generalize across domains and boost high-level scene understanding tasks, several unsupervised pre-training works are proposed for scene-level 3D tasks. Considering that PointContrast focuses on point-level alignment without capturing spatial configurations and contexts in scenes, Hou *et al.* [3] integrated spatial contexts into the pre-training objective by partitioning the space into spatially

inhomogeneous cells for correspondence matching. Hou *et al.* [112] built a multi-modal contrastive learning framework that models 2D multi-view correspondences as well as 2D-3D correspondences with geometry-to-image alignment. While the aforementioned works [3], [48], [112] require 3D data captured from multiple camera views, Zhang *et al.* [97] proposed DepthContrast that can work with single-view data. Instead of using real point clouds as previous methods, Rao *et al.* [96] generated synthetic scenes and objects from ShapeNet [14] for network pre-training.

Another unsupervised approach to learn context similarity is *clustering*. In this approach, samples are first grouped into clusters by clustering algorithms such as K-Means [113] and each sample is assigned a cluster ID as pseudo-label. Then networks are trained in a supervised manner to learn semantic structures of data distribution. The learned parameters are used for model initialization for fine-tuning various downstream tasks. A typical example is Deep-Clustering [114] which is the first unsupervised clustering method for 2D visual representation learning. However, no prior studies adopted a purely clustering strategy for URL of point clouds. Instead, hybrid approaches are proposed by integrating clustering with other unsupervised learning approaches (e.g., self-reconstruction [89] or contrastive learning [90]) for learning more robust representations.

### 5.2.2 Learning with spatial context structure

Point-cloud data consisting of spatial coordinates provide accurate geometric descriptions for the 3D shapes of objects and scenes. The rich spatial contexts in point-cloud data can also be exploited in pre-text tasks for representation learning. For example, the networks can be trained to sort out the relations among different parts of objects. Likewise, the learned parameters can be used as model initialization for downstream tasks. Since no human annotations are required in training, the key is to design effective pre-text tasks to exploit spatial contexts as the unsupervised training objectives.

The method Jigsaw3D [13] proposed by Sauder *et al.* is one of the pioneer works that use spatial context for URL of point clouds. As illustrated in Fig. 18, objects are first split into voxels where each point is assigned a voxel

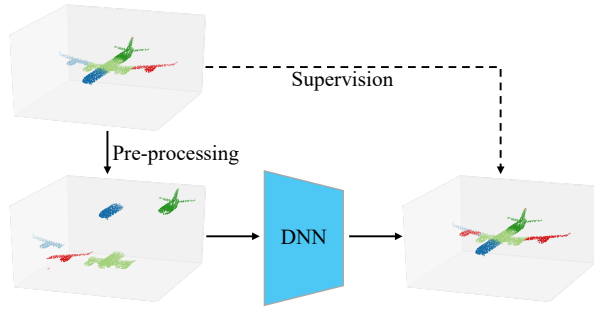


Fig. 18: The pipeline of 3DJigsaw [13]: An object is split into voxels where each point is assigned with a voxel label. The split voxels are randomly rearranged via pre-processing, and a deep neural network is trained to predict the voxel label for each point. The graph is reproduced based on [13].

label. The network is then fed with randomly rearranged point clouds and optimized by predicting correct voxel label for each point. During the training, the network aims to extract spatial relations and geometric information from point clouds. In their following work [115], another pre-text task was designed to predict one of ten spatial relationships of two local parts from the same object. Inspired by the 2D method that predicts image rotations [116], Poursaeed *et al.* [94] proposed to learn representations by predicting rotation angles of 3D objects. Thabet *et al.* [117] designed a pre-text task that predicts the next point in a point sequence defined by Morton-order Space Filling Curve. Chen *et al.* [98] proposed to learn the spatial context of objects by distinguishing the distorted parts of a shape from the correct ones. Sun *et al.* [118] introduced a mix-and-disentangle task to exploit spatial context cues.

### 5.2.3 Learning with temporal context structure

Point cloud sequence is a common type of point cloud data that consists of consecutive point cloud frames similar to video data. For example, there are indoor point cloud sequences transformed from RGB-D video frames [16] and LiDAR sequential data [17], [119], [120] consisting of continuous point cloud scans where each scan is collected by one sweep of LiDAR sensors. Point cloud sequences contain rich temporal information that can be extracted by designing pre-text tasks and used as supervision signals to train DNNs. The learned representations can be transferred to downstream tasks.

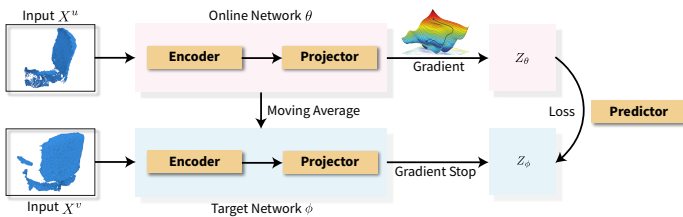


Fig. 19: The pipeline of STRL [1]: An Online Network learns spatial and temporal structures from two neighbouring point cloud frames  $X^u$  and  $X^v$ . The figure is adopted from [1] with authors' permission.

Recently, Huang *et al.* [1] proposed a framework Spatio-Temporal Representation Learning (STRL) as illustrated in Fig. 19. STRL extends BYOL [8] from 2D vision to 3D vision and extracts spatial and temporal representation from point clouds. Specifically, it treats two neighboring point cloud frames as positive pairs and minimizes the mean squared error between the learned feature representations of sample pairs. Chen *et al.* [121] exploit synthetic 3D shapes moving in static 3D environments to create dynamic scenarios and sample pairs in the temporal order. They then conducted contrastive learning to learn 3D representations with dynamic understanding.

Unsupervised learning with temporal context structures has proved its effectiveness in both 2D computer vision tasks [122], [123], [124], [125] and 3D computer vision tasks [1], [121]. As discussed in Section 7, this direction is very promising but more research and development are needed for better harvesting the temporal contextual information.

### 5.2.4 Summary and discussion

Learning context information including context similarity, spatial context structure, and temporal context structure is a rising research direction for URL of point clouds. While a majority of URL methods for point clouds are designed for object-level representation learning, several latest context-based works [1], [47], [48], [97] have demonstrated that the learned representations can generalize across domains and boost performances of different scene-level tasks. These findings inspire the research of URL of point clouds and encourage more research on unsupervised pre-text design for 3D deep representation learning.

## 5.3 Multiple modal-based methods

Different modalities such as images [17] and natural language descriptions [126] can provide additional information for point-cloud data. Modeling relationships across modalities can be designed as pre-text tasks for URL which helps networks to learn more robust and comprehensive representations. Likewise, the learned parameters can be used as initialization weights for various downstream tasks.

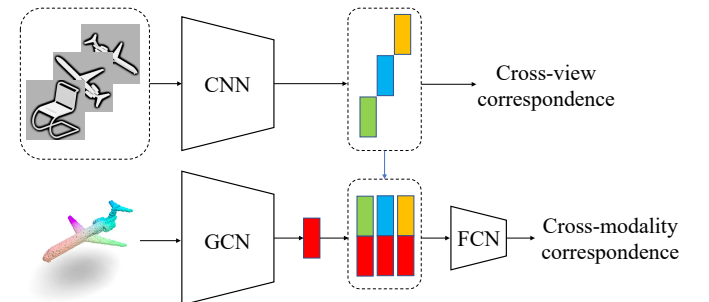


Fig. 20: The pipeline of CMCV [4]: CMCV employs a 2D CNN to extract 2D image features from rendered views of 3D objects and a 3D GCN to extract 3D features from point clouds directly. The two types of features are then concatenated by a two-layer fully connected network (FCN) to predict cross-modality correspondences. The graph is reproduced based on [4].

Recent works [4], [130] exploited the correspondences across 3D point cloud objects and 2D images for unsupervised representation learning. For example, Jing *et al.* [4] render 3D objects with different camera views into 2D images for learning from multi-modality data. As Fig. 20 shows, they employ a 2D CNN and a 3D GCN to extract image features and point cloud features, respectively, and then conduct contrastive learning on intra-modal correspondences and cross-modal correspondences. Their study shows that both pre-trained 2D CNN and 3D GCN achieved better classification results as compared with random initialization. However, how to learn unsupervised point cloud representations with other modalities such as text descriptions and audio data remains an under-explored field. We expect more

studies in this promising research direction.

#### 5.4 Local descriptor-based methods

The aforementioned methods aim to learn semantic structures of point clouds for high-level understanding, while the local descriptor-based methods focus on learning representations for low-level tasks. For example, Deng *et al.* [131] introduced PPF-FoldNet that extracts rotation-invariant 3D local descriptors for 3D matching [132]. Several works [133], [134] exploit non-rigid shape correspondence extraction as pre-text tasks for URL of point clouds, aiming to find the point-to-point correspondence of two deformable 3D shapes. Jiang *et al.* [135] explore unsupervised 3D registra-

TABLE 4: Comparisons of linear shape classification performance on datasets ModelNet10 and ModelNet40 [27]: The linear SVM classifiers are trained with the representations learned by different unsupervised methods. The accuracy numbers highlighted by \* represent results of pre-training with multi-modal data.

Method	Year	Pre-text task	Backbone	Pre-train dataset	ModelNet10	ModelNet40
Supervised learning	2017	N.A.	PointNet [15]	N.A.	-	89.2
	2017		PointNet++ [42]		-	90.7
	2019		DGCNN [45]		-	93.5
	2019		RSCNN [50]		-	93.6
SPH [127]	2003	Generation	-	ShapeNet	79.8	68.2
LFD [128]	2003	Generation	-	ShapeNet	79.9	75.5
TL-Net [58]	2016	Generation	-	ShapeNet	-	74.4
VConv-DAE [57]	2016	Generation	-	ShapeNet	80.5	75.5
3D-GAN [59]	2016	Generation	-	ShapeNet	91.0	83.3
3D DescriptorNet [60]	2018	Generation	-	ShapeNet	-	92.4
FoldingNet [61]	2018	Generation	-	ModelNet40	91.9	84.4
FoldingNet [61]	2018	Generation	-	ShapeNet	94.4	88.4
Latent-GAN [63]	2018	Generation	-	ModelNet40	92.2	87.3
Latent-GAN [63]	2018	Generation	-	ShapeNet	95.3	85.7
MRTNet [64]	2018	Generation	-	ShapeNet	86.4	-
VIP-GAN [65]	2019	Generation	-	ShapeNet	94.1	92.0
3DCapsuleNet [41]	2019	Generation	-	ShapeNet	-	88.9
PC-GAN [81]	2019	Generation	-	ModelNet40	-	87.8
L2G-AE [66]	2019	Generation	-	ShapeNet	95.4	90.6
MAP-VAE [67]	2019	Generation	-	ShapeNet	94.8	90.2
PointFlow [68]	2019	Generation	-	ShapeNet	93.7	86.8
MultiTask [89]	2019	Hybrid	-	ShapeNet	-	89.1
Jigsaw3D [13]	2019	Context	PointNet	ShapeNet	91.6	87.3
Jigsaw3D [13]	2019	Context	DGCNN	ShapeNet	94.5	90.6
ClusterNet [90]	2019	Context	DGCNN	ShapeNet	93.8	86.8
CloudContext [115]	2019	Context	DGCNN	ShapeNet	94.5	89.3
NeuralSampler [83]	2019	Generation	-	ShapeNet	95.3	88.7
PointGrow [72]	2020	Generation	-	ShapeNet	85.8	-
Info3D [92]	2020	Context	PointNet	ShapeNet	-	89.8
Info3D [92]	2020	Context	DGCNN	ShapeNet	-	91.6
ACD [93]	2020	Context	PointNet++	ShapeNet	-	89.8
PDL [69]	2020	Generation	-	ShapeNet	-	84.7
GLR [91]	2020	Hybrid	PointNet++	ShapeNet	94.8	92.2
GLR [91]	2020	Hybrid	RSCNN	ShapeNet	94.6	92.2
SA-Net-cls [71]	2020	Generation	-	ShapeNet	-	90.6
GraphTER [70]	2020	Generation	-	ModelNet40	-	89.1
Rotation3D [94]	2020	Context	PointNet	ShapeNet	-	88.6
Rotation3D [94]	2020	Context	DGCNN	ShapeNet	-	90.8
MID [110]	2020	Context	HRNet	ShapeNet	-	90.3
GTIF [78]	2020	Generation	HRNet	ShapeNet	95.9	89.6
HNS [95]	2021	Context	DGCNN	ShapeNet	-	89.6
ParAE [129]	2021	Generation	PointNet	ShapeNet	-	90.3
ParAE [129]	2021	Generation	DGCNN	ShapeNet	-	91.6
CMCV [4]	2021	Multi-modal	DGCNN	ShapeNet	-	89.8*
GSIR [79]	2021	Context	DGCNN	ModelNet40	-	90.4
STRL [1]	2021	Context	PointNet	ShapeNet	-	88.3
STRL [1]	2021	Context	DGCNN	ShapeNet	-	90.9
PSG-Net [73]	2021	Generation	PointNet++	ShapeNet	-	90.9
SelfCorrection [98]	2021	Hybrid	PointNet	ShapeNet	93.3	89.9
SelfCorrection [98]	2021	Hybrid	RSCNN	ShapeNet	95.0	92.4
CrossPoint [130]	2022	Multi-modal	PointNet	ShapeNet	-	89.1*
CrossPoint [130]	2022	Multi-modal	DGCNN	ShapeNet	-	91.2*

tion for finding the optimal rigid transformation that can align the source point cloud to the target precisely.

The performances of existing local descriptor-based methods are mainly evaluated on low-level tasks. However, how to adapt learned feature representations toward other high-level tasks is rarely discussed. We expect more related research in the future.

## 6 BENCHMARK PERFORMANCES

This section compares the performances of unsupervised representation learning methods on public point clouds datasets. As introduced in Section 2.2, the quality of unsupervised representations is often evaluated on downstream tasks including object-level tasks (e.g., object classification and object part segmentation) and scene-level tasks (e.g., semantic segmentation, instance segmentation and object detection). We summarize the performance of the existing works by tasks and compare them in the rest of this section.

### 6.1 Object-level tasks

#### 6.1.1 Object classification

Object classification is the most widely used downstream task in evaluations since the majority of existing works learn point cloud representations on object-level datasets. As described in Section 2.2.1, two types of classification protocols are widely adopted including the linear classification protocol and the fine-tuning protocol.

Table 4 summarizes the performance of the linear classification over ModelNet10 and ModelNet40 by existing methods. In this protocol, linear classifiers are trained with the representations learned by different unsupervised methods on the ShapeNet or ModelNet40 dataset. We also list supervised learning performances for benchmarking. It can be seen that the performances of unsupervised learning methods keep improving and some methods have even surpassed supervised learning methods, demonstrating the effectiveness and great potential of URL of point clouds.

Another evaluation protocol is fine-tuning unsupervised learned models over object classification task. Table 5 lists

TABLE 5: Comparisons of unsupervised pre-training performance over the object classification datasets ModelNet40 and OBJ-BG split in ScanObjectNN. Metric "A/B": "A" represents training from scratch while "B" represents unsupervised pre-training.

Method	Backbone	ModelNet40	ScanObjectNN
Jigsaw3D [13]	PointNet [15]	89.2/89.6(+0.4)	73.5/76.5(+3.0)
Info3D [92]	PointNet [15]	89.2/90.2(+1.0)	-/-
SelfCorrection [98]	PointNet [15]	89.1/90.0(+0.9)	-/-
OcCo [12]	PointNet [15]	89.2/90.1(+0.9)	73.5/80.0(+6.5)
ParAE [129]	PointNet [15]	89.2/90.5(+1.3)	-/-
Jigsaw3D [13]	PCN [100]	89.3/89.6(+0.3)	78.3/78.2(-0.1)
OcCo [12]	PCN [100]	89.3/90.3(+1.0)	78.3/80.4(+2.1)
GLR [91]	RSCNN [50]	91.8/92.2(+0.5)	-/-
SelfCorrection [98]	RSCNN [50]	91.7/93.0(+1.3)	-/-
Jigsaw3D [13]	DGCNN [45]	92.2/92.4(+0.2)	82.4/82.7(+0.3)
Info3D [92]	DGCNN [45]	93.5/93.0(-0.5)	-/-
OcCo [12]	DGCNN [45]	92.5/93.0(+0.5)	82.4/83.9(+1.6)
ParAE [129]	DGCNN [45]	92.2/92.9(+0.7)	-/-
STRL [1]	DGCNN [45]	92.2/93.1(+0.9)	-/-
OcCo [12]	Transformer [56]	91.2/92.2(+1.0)	79.9/84.9(+5.0)
Point-BERT [56]	Transformer [56]	91.2/93.4(+2.2)	79.9/87.4(+7.5)

the performances on the ModelNet40 and ScanObjectNN datasets. We can see that classification models initialized with unsupervised pre-trained weights always achieve better classification performances as compared with random initialization, regardless of backbone architectures. On the other hand, the performance gaps are still limited, largely due to the limited size and diversity of the pre-training datasets (i.e., ShapeNet and ModelNet40) and the simplicity of existing backbone models. In comparison, thanks to the much larger pre-training datasets ImageNet [33] and the more powerful backbone network ResNet [37], the state-of-the-art methods for unsupervised pre-training of 2D images are able to achieve more significant performance gains in the classification task. As discussed in Section 7, we expect more diverse datasets and more advanced and generous backbone models that can set stronger foundations for this field.

#### 6.1.2 Object part segmentation

Table 6 lists the performances of object part segmentation over the ShapeNetPart dataset [14]. As defined in Section 2.2.2, we summarize the mIoU over instances and mIoU over categories on the test set. Similar to object classification, there are two different setups that are often used for the evaluation of object part segmentation. The linear classification protocol requires training a linear classifier with point features that are learned by unsupervised methods. The segmentation results over the test set are reported as the type "Unsup." in Table 6. The fine-tuning protocol initializes segmentation networks with unsupervised pre-trained weights and re-trains models in a supervised manner. Segmentation results are shown in the type "Trans." in Table 6. It can be seen that the performance gap between unsupervised learning and supervised learning is narrowing ("Unsup." v.s. "Sup."). In addition, the knowledge from unsupervised

TABLE 6: Comparisons of shape part segmentation on dataset ShapeNetPart [14]. "Sup." represents training segmentation models from scratch in a supervised manner; "Unsup." means training a linear classifier over the unsupervised point features; "Trans." represents fine-tuning segmentation models (that are initialized with the unsupervised pre-trained models) in a supervised manner.

URL Method	Type	Backbone	class mIoU	instance mIoU
N.A.	Sup.	PointNet	80.4	83.7
	Sup.	PointNet++	81.9	85.1
	Sup.	DGCNN	82.3	85.1
	Sup.	RSCNN	84.0	86.2
	Sup.	Transformer	83.4	85.1
Latent-GAN [63]	Unsup.	-	57.0	-
MAP-VAE [67]	Unsup.	-	68.0	-
CloudContext [115]	Unsup.	DGCNN	-	81.5
GraphTER [70]	Unsup.	-	78.1	81.9
MID [110]	Unsup.	HRNet	83.4	84.6
HNS [95]	Unsup.	DGCNN	79.9	82.3
CMCV [4]	Unsup.	DGCNN	74.7	80.8
SO-Net [62]	Trans.	SO-Net	-/-	84.6/84.9(+0.3)
Jigsaw3D [13]	Trans.	DGCNN	82.3/83.1(+0.8)	85.1/85.3(+0.2)
MID [110]	Trans.	HRNet	84.6/85.2(+0.6)	85.5/85.8(+0.3)
CMCV [4]	Trans.	DGCNN	77.6/79.1(+1.5)	83.0/83.7(+0.7)
OcCo [12]	Trans.	PointNet	82.2/83.4(+1.2)	-/-
OcCo [12]	Trans.	DGCNN	84.4/85.0(+0.6)	-/-
OcCo [12]	Trans.	Transformer	83.4/83.4(+0.0)	85.1/85.1(+0.0)
Point-BERT [56]	Trans.	Transformer	83.4/84.1(+0.7)	85.1/85.6(+0.5)

TABLE 7: Semantic segmentation on dataset S3DIS [21]: It shows comparisons between supervised training with random weight initialization and with pre-trained weights learned from unsupervised pre-training tasks. It uses DGCNN as the segmentation model, which is trained on different single Areas and tested on Area 5 (upper part) and Area 6 (lower part).

Method	OA on area 5 with different train area					mIoU on area 5 with different train area				
	Area1	Area2	Area3	Area4	Area6	Area1	Area2	Area3	Area4	Area6
<i>from scratch</i>	82.9	81.2	82.8	82.8	83.1	43.6	34.6	39.9	39.4	43.9
Jigsaw3D [13]	83.5(+0.6)	81.2(+0.0)	84.0(+1.2)	82.9(+0.1)	83.3(+0.2)	44.7(+1.1)	34.9(+0.3)	42.4(+2.5)	39.9(+0.5)	43.9(+0.0)
ParAE [129]	91.8(+8.9)	82.3(+1.1)	89.5(+6.7)	88.2(+5.4)	86.4(+3.3)	53.5(+9.9)	38.5(+3.9)	48.4(+8.5)	45.0(+5.6)	49.2(+5.3)

Method	OA on area 6 with different train area					mIoU on area 6 with different train area				
	Area1	Area2	Area3	Area4	Area5	Area1	Area2	Area3	Area4	Area5
<i>from scratch</i>	84.6	70.6	77.7	73.6	76.9	57.9	38.9	49.5	38.5	48.6
STRL [1]	85.3(+0.7)	72.4(+1.8)	79.1(+1.4)	73.8(+0.2)	77.3(+0.4)	59.2(+1.3)	39.2(+0.8)	51.9(+2.4)	39.3(+0.8)	49.5(+0.9)

TABLE 8: Performances for semantic segmentation on S3DIS [21]. Upper part: Models are tested on Area5 (Fold#1) and trained on the rest of the data. Lower part: Six-fold cross-validation over three runs.

Method	Backbone	mACC	mIoU
<i>from scratch</i>	SR-UNet	75.5	68.2
PointContrast [48]		77.0	70.9
DepthContrast [97]		-	70.6

Method	Backbone	OA	mIoU
<i>from scratch</i>	PointNet	78.2	47.0
Jigsaw3D [13]		80.1	52.6
OcOc [12]		82.0	54.9
<i>from scratch</i>	PCN	82.9	51.1
Jigsaw3D [13]		83.7	52.2
OcOc [12]		85.1	53.4
<i>from scratch</i>	DGCNN	83.7	54.9
Jigsaw3D [13]		84.1	55.6
OcOc [12]		84.6	58.0

learning helps to train better object part segmentation models in most cases but the performance gains are still limited ("Trans." v.s. "Sup.").

## 6.2 Scene-level tasks

As described in Section 5.2, another newly rising research direction in URL of point clouds is unsupervised pre-training on scene-level point clouds (e.g., ScanNet dataset) and fine-tuning networks for scene-level tasks including semantic segmentation, instance semantic segmentation, and object detection.

Tables 7 and 8 show the performances of semantic segmentation on the S3DIS [21] dataset. We summarized them separately since different fine-tuning setups have been used in prior works. In Table 7, the unsupervised pre-trained DGCNN is fine-tuned on every *single area* of S3DIS and tested on either Area 5 (the upper part of table) or Area 6 (the lower part of the table). Table 8 instead shows the performance of fine-tuning different segmentation networks with the *whole* dataset by following the one-fold (in the upper part of the table) and six-fold cross-validation setups (in the lower part of the table), respectively.

We also summarize existing works that handle unsupervised pre-training for object detection. Tables 9 and 10 show their performances over indoor datasets including SUN RGB-D [28] and ScanNet-V2 [16] as well as outdoor LiDAR dataset ONCE [30], respectively. In addition, several works investigated unsupervised pre-training for instance segmentation. We summarize their performance over S3DIS [21] and ScanNet-V2 [16] in Table 11.

TABLE 9: Comparison of pre-training effects by different unsupervised learning methods. The benchmarking is 3D object detection task over datasets SUN RGB-D [28] and ScanNet-V2 [16]. "@0.25" and "@0.5" represent per-category results of average precision (AP) with IoU threshold 0.25 (mAP@0.25) and 0.5 (mAP@0.5), respectively.

Method	Backbone	SUN RGB-D		ScanNet-V2	
		@0.5	@0.25	@0.5	@0.25
<i>from scratch</i>	SR-UNet	31.7	55.6	35.4	56.7
PointContrast [48]		34.8	57.5	38.0	58.5
<i>from scratch</i>	VoteNet	32.9	57.7	33.5	58.6
STRL [1]		-	58.2	-	-
RandRooms [96]		35.4	59.2	36.2	61.3
DepthContrast [97]		-	-	-	62.2
CSC [3]		33.6	-	-	-
PointContrast [48]		34.0	-	38.0	-
4DContrast [121]		34.4	-	39.3	-
<i>from scratch</i>	PointNet++	-	57.5	-	58.6
PointContrast [48]		-	57.9	-	58.5
RandRooms [96]		-	59.2	-	61.3
DepthContrast [97]		-	60.7	-	-
<i>from scratch</i>	H3DNet	39.0	60.1	48.1	67.3
RandRooms [96]		43.1	61.6	51.5	68.6

TABLE 10: Object detection performance on dataset ONCE [30]. The baseline is trained from scratch. Unsupervised learning methods are used for pre-training models.  $U_{small}$ ,  $U_{median}$ , and  $U_{large}$  represent small, medium, and large amounts of unlabelled data that are used for unsupervised learning, respectively.

Method	Vehicle	Pedestrian	Cyclist	mAP
Baseline [136]	69.7	26.1	59.9	51.9

$U_{small}$				
BYOL [8]	67.6	17.2	53.4	46.1 (-5.8)
PointContrast [48]	71.5	22.7	58.0	50.8 (-0.1)
SwAV [137]	72.3	25.1	60.7	52.7 (+0.8)
DeepCluster [114]	72.1	27.6	50.3	53.3 (+1.4)

$U_{median}$				
BYOL [8]	69.7	27.3	57.2	51.4 (-0.5)
PointContrast [48]	70.2	29.2	58.9	52.8 (+0.9)
SwAV [137]	72.1	28.0	60.2	53.4 (+1.5)
DeepCluster [114]	72.1	30.1	60.5	54.2 (+2.3)

$U_{large}$				
BYOL [8]	72.2	23.6	60.5	52.1 (+0.2)
PointContrast [48]	73.2	27.5	58.3	53.0 (+1.1)
SwAV [137]	72.0	30.6	60.3	54.3 (+2.4)
DeepCluster [114]	71.9	30.5	60.4	54.3 (+2.4)

It is inspiring to see that unsupervised learning representation can generalize across domains and boost performances over multiple high-level 3D tasks as compared with training from scratch. These experiments demonstrate the huge potential of URL of point clouds in saving expensive

TABLE 11: Performances of instance segmentation on datasets S3DIS [21] and ScanNet-V2 [16]. It reports the mean of average precision (mAP) across all semantic classes with a 3D IoU threshold of 0.25.

Method	Backbone	S3DIS	ScanNet
<i>from scratch</i>		59.3	53.4
PointContrast [48]	SR-UNet	60.5	55.8
CSC [3]		63.4	56.5
4DContrast [121]		-	57.6

human annotations. However, the improvements are still limited and we expect more research in this area.

## 7 FUTURE DIRECTION

URL of point clouds has achieved significant progress during the last decade. We share several potential future research directions of this research field in this section.

**Unified 3D backbones are needed:** One major reason of the great success of deep learning in 2D computer vision is the standardization of CNN architectures with classical examples such as VGG [36] and ResNet [37]. For example, the unified backbone structures greatly facilitate knowledge transfer across different datasets and tasks. For 3D point clouds, the development of similarly unified 3D backbones is instead far under-explored, despite a variety of 3D deep architectures that have been designed over the last few years. This can be observed from the URL methods in Tables 4, 5, 6, 8, 9 in Section 6 most of which adopted very different backbone models. This impedes the development of 3D point cloud networks in terms of scalable designs, efficient deployment in various practical applications, etc. Designing certain universal backbones that can be as ubiquitous as ResNet in 2D computer vision is crucial for the advance of 3D point cloud networks including unsupervised point cloud representation learning.

**Larger datasets are needed:** As described in Section 3, most existing datasets in unsupervised representation learning were originally collected for the task of supervised learning. Since point cloud annotation is laborious and time-consuming, these datasets are severely constrained in data size and data diversity and are not suitable for unsupervised point cloud representation learning which usually requires large amounts of point clouds of good size and diversity. The limitation of existing datasets largely explains the insignificant performance improvements of unsupervised pre-training in Tables 5, 6, 7, 8, 9, 10, 11. To address this critical issue, it is urgent to collect large-scale and high-quality point cloud datasets of sufficient diversity in terms of object-level and scene-level point clouds, indoor and outdoor point clouds, etc.

**Unsupervised pre-training for scene-level tasks:** As described in Section 5.2, most earlier point cloud research focuses on object-level point cloud processing though several pioneer studies [1], [3], [48], [96], [112] explored how to pre-train DNNs on scene-level point clouds for improving various scene-level downstream tasks such as object detection and instance segmentation. The pioneer studies have demonstrated that the learned unsupervised representations can effectively generalize across domains and tasks. Hence, URL of scene-level point clouds deserves more attention as

a new direction due to its great potential in a variety of applications. On the other hand, the research in along this line remains at a nascent stage, largely due to the constraints in network architectures and datasets. We foresee that more useful research will be carried out on unsupervised learning from scene-level point clouds.

**Learning representations from multi-modal data:** 3D sensors are often equipped with other types of sensors that can capture additional and complementary information to point clouds. For example, depth cameras are often equipped with optical sensor for capturing better appearance information. LiDAR sensor, optical sensors, GPU, and IMU are often equipped together as a sensor suite to capture complementary information and also provide certain redundancy in autonomous vehicles and mobile robot navigation. Unsupervised learning from such multi-modal data has attracted some attention in recent years. For example, learning correspondences among multi-modal data from different sensors has been explored as pre-text tasks for unsupervised learning as described in Section 5.3. However, the study along this line of research remains under-investigated and we expect more research on unsupervised learning from multi-modal data including point clouds, 2D RGB images, depth maps, etc.

**Learning Spatio-temporal representations:** 3D sensors that support capturing sequential point clouds are becoming increasingly popular nowadays. Rich temporal information from point cloud streams can be extracted as useful supervision signals for unsupervised learning while most of the existing works still focus on static point clouds. We expect that more effective pretext tasks will be designed that can effectively learn spatio-temporal representations from unlabelled sequential point cloud frames.

## 8 CONCLUSION

Unsupervised representation learning aims to learn effective representations from unannotated data, which has demonstrated impressive progress and promising applications in the research with point cloud data. This paper presents a contemporary survey of unsupervised representation learning of point clouds. It first introduced the widely adopted datasets and deep network architectures. A comprehensive taxonomy and detailed review of methods are then presented. Following that, representative methods are discussed and benchmarked over multiple 3D point cloud tasks. Finally, we share our humble opinions about several potential future research directions. We hope that this work can lay a strong and sound foundation for the future research in unsupervised representation learning from point cloud data.

## ACKNOWLEDGMENTS

This study is supported under the RIE2020 Industry Alignment Fund – Industry Collaboration Projects (IAF-ICP) Funding Initiative, as well as cash and in-kind contribution from Singapore Telecommunications Limited (Singtel), through Singtel Cognitive and Artificial Intelligence Lab for Enterprises (SCALE@NTU).

## REFERENCES

- [1] S. Huang, Y. Xie, S.-C. Zhu, and Y. Zhu, "Spatio-temporal self-supervised representation learning for 3d point clouds," in *Proceedings of the IEEE/CVF International Conference on Computer Vision*, 2021, pp. 6535–6545.
- [2] Y. Guo, H. Wang, Q. Hu, H. Liu, L. Liu, and M. Bennamoun, "Deep learning for 3d point clouds: A survey," *IEEE transactions on pattern analysis and machine intelligence*, 2020.
- [3] J. Hou, B. Graham, M. Nießner, and S. Xie, "Exploring data-efficient 3d scene understanding with contrastive scene contexts," in *Proceedings of the IEEE/CVF Conference on Computer Vision and Pattern Recognition*, 2021, pp. 15587–15597.
- [4] L. Jing, L. Zhang, and Y. Tian, "Self-supervised feature learning by cross-modality and cross-view correspondences," in *Proceedings of the IEEE/CVF Conference on Computer Vision and Pattern Recognition*, 2021, pp. 1581–1591.
- [5] A. Radford, J. Wu, R. Child, D. Luan, D. Amodei, I. Sutskever *et al.*, "Language models are unsupervised multitask learners," *OpenAI blog*, vol. 1, no. 8, p. 9, 2019.
- [6] J. D. M.-W. C. Kenton and L. K. Toutanova, "Bert: Pre-training of deep bidirectional transformers for language understanding," in *Proceedings of NAACL-HLT*, 2019, pp. 4171–4186.
- [7] K. He, H. Fan, Y. Wu, S. Xie, and R. Girshick, "Momentum contrast for unsupervised visual representation learning," in *Proceedings of the IEEE/CVF Conference on Computer Vision and Pattern Recognition*, 2020, pp. 9729–9738.
- [8] J.-B. Grill, F. Strub, F. Altché, C. Tallec, P. Richemond, E. Buchatskaya, C. Doersch, B. Pires, Z. Guo, M. Azar *et al.*, "Bootstrap your own latent: A new approach to self-supervised learning," in *Neural Information Processing Systems*, 2020.
- [9] X. Chen, H. Fan, R. Girshick, and K. He, "Improved baselines with momentum contrastive learning," *arXiv preprint arXiv:2003.04297*, 2020.
- [10] K. He, X. Chen, S. Xie, Y. Li, P. Dollár, and R. Girshick, "Masked autoencoders are scalable vision learners," *arXiv preprint arXiv:2111.06377*, 2021.
- [11] D. Valsesia, G. Fracastoro, and E. Magli, "Learning localized generative models for 3d point clouds via graph convolution," in *International conference on learning representations*, 2018.
- [12] H. Wang, Q. Liu, X. Yue, J. Lasenby, and M. J. Kusner, "Unsupervised point cloud pre-training via occlusion completion," in *Proceedings of the IEEE/CVF International Conference on Computer Vision (ICCV)*, October 2021, pp. 9782–9792.
- [13] J. Sauder and B. Sievers, "Self-supervised deep learning on point clouds by reconstructing space," *Advances in Neural Information Processing Systems*, vol. 32, pp. 12962–12972, 2019.
- [14] A. X. Chang, T. Funkhouser, L. Guibas, P. Hanrahan, Q. Huang, Z. Li, S. Savarese, M. Savva, S. Song, H. Su *et al.*, "Shapenet: An information-rich 3d model repository," *arXiv preprint arXiv:1512.03012*, 2015.
- [15] C. R. Qi, H. Su, K. Mo, and L. J. Guibas, "Pointnet: Deep learning on point sets for 3d classification and segmentation," in *Proceedings of the IEEE conference on computer vision and pattern recognition*, 2017, pp. 652–660.
- [16] A. Dai, A. X. Chang, M. Savva, M. Halber, T. Funkhouser, and M. Nießner, "ScanNet: Richly-annotated 3d reconstructions of indoor scenes," in *Proceedings of the IEEE conference on computer vision and pattern recognition*, 2017, pp. 5828–5839.
- [17] A. Geiger, P. Lenz, C. Stiller, and R. Urtasun, "Vision meets robotics: The kitti dataset," *The International Journal of Robotics Research*, vol. 32, no. 11, pp. 1231–1237, 2013.
- [18] C. R. Qi, O. Litany, K. He, and L. J. Guibas, "Deep hough voting for 3d object detection in point clouds," in *Proceedings of the IEEE/CVF International Conference on Computer Vision*, 2019, pp. 9277–9286.
- [19] C. R. Qi, W. Liu, C. Wu, H. Su, and L. J. Guibas, "Frustum pointnets for 3d object detection from rgb-d data," in *Proceedings of the IEEE conference on computer vision and pattern recognition*, 2018, pp. 918–927.
- [20] S. Shi, X. Wang, and H. Li, "Pointcnn: 3d object proposal generation and detection from point cloud," in *Proceedings of the IEEE/CVF conference on computer vision and pattern recognition*, 2019, pp. 770–779.
- [21] I. Armeni, O. Sener, A. R. Zamir, H. Jiang, I. Brilakis, M. Fischer, and S. Savarese, "3d semantic parsing of large-scale indoor spaces," in *Proceedings of the IEEE Conference on Computer Vision and Pattern Recognition*, 2016, pp. 1534–1543.
- [22] A. Ioannidou, E. Chatzilari, S. Nikolopoulos, and I. Kompatsiaris, "Deep learning advances in computer vision with 3d data: A survey," *ACM Computing Surveys (CSUR)*, vol. 50, no. 2, pp. 1–38, 2017.
- [23] Y. Xie, J. Tian, and X. X. Zhu, "Linking points with labels in 3d: A review of point cloud semantic segmentation," *IEEE Geoscience and Remote Sensing Magazine*, vol. 8, no. 4, pp. 38–59, 2020.
- [24] L. Jing and Y. Tian, "Self-supervised visual feature learning with deep neural networks: A survey," *IEEE transactions on pattern analysis and machine intelligence*, 2020.
- [25] X. Liu, F. Zhang, Z. Hou, L. Mian, Z. Wang, J. Zhang, and J. Tang, "Self-supervised learning: Generative or contrastive," *IEEE Transactions on Knowledge and Data Engineering*, 2021.
- [26] G.-J. Qi and J. Luo, "Small data challenges in big data era: A survey of recent progress on unsupervised and semi-supervised methods," *IEEE Transactions on Pattern Analysis and Machine Intelligence*, 2020.
- [27] Z. Wu, S. Song, A. Khosla, F. Yu, L. Zhang, X. Tang, and J. Xiao, "3d shapenets: A deep representation for volumetric shapes," in *Proceedings of the IEEE conference on computer vision and pattern recognition*, 2015, pp. 1912–1920.
- [28] S. Song, S. P. Lichtenberg, and J. Xiao, "Sun rgb-d: A rgb-d scene understanding benchmark suite," in *Proceedings of the IEEE conference on computer vision and pattern recognition*, 2015, pp. 567–576.
- [29] M. A. Uy, Q.-H. Pham, B.-S. Hua, T. Nguyen, and S.-K. Yeung, "Revisiting point cloud classification: A new benchmark dataset and classification model on real-world data," in *Proceedings of the IEEE/CVF International Conference on Computer Vision*, 2019, pp. 1588–1597.
- [30] J. Mao, M. Niu, C. Jiang, H. Liang, J. Chen, X. Liang, Y. Li, C. Ye, W. Zhang, Z. Li *et al.*, "One million scenes for autonomous driving: Once dataset," *arXiv preprint arXiv:2106.11037*, 2021.
- [31] G. Ros, L. Sellart, J. Materzynska, D. Vazquez, and A. M. Lopez, "The synthia dataset: A large collection of synthetic images for semantic segmentation of urban scenes," in *Proceedings of the IEEE conference on computer vision and pattern recognition*, 2016, pp. 3234–3243.
- [32] J. Devlin, M.-W. Chang, K. Lee, and K. Toutanova, "Bert: Pre-training of deep bidirectional transformers for language understanding," *arXiv preprint arXiv:1810.04805*, 2018.
- [33] J. Deng, W. Dong, R. Socher, L.-J. Li, K. Li, and L. Fei-Fei, "Imagenet: A large-scale hierarchical image database," in *2009 IEEE conference on computer vision and pattern recognition*. Ieee, 2009, pp. 248–255.
- [34] A. Hornung, K. M. Wurm, M. Bennewitz, C. Stachniss, and W. Burgard, "Octomap: An efficient probabilistic 3d mapping framework based on octrees," *Autonomous robots*, vol. 34, no. 3, pp. 189–206, 2013.
- [35] M. Nießner, M. Zollhöfer, S. Izadi, and M. Stamminger, "Real-time 3d reconstruction at scale using voxel hashing," *ACM Transactions on Graphics (ToG)*, vol. 32, no. 6, pp. 1–11, 2013.
- [36] K. Simonyan and A. Zisserman, "Very deep convolutional networks for large-scale image recognition," *arXiv preprint arXiv:1409.1556*, 2014.
- [37] K. He, X. Zhang, S. Ren, and J. Sun, "Deep residual learning for image recognition," in *Proceedings of the IEEE conference on computer vision and pattern recognition*, 2016, pp. 770–778.
- [38] H. Su, S. Maji, E. Kalogerakis, and E. Learned-Miller, "Multi-view convolutional neural networks for 3d shape recognition," in *Proceedings of the IEEE international conference on computer vision*, 2015, pp. 945–953.
- [39] A. Xiao, X. Yang, S. Lu, D. Guan, and J. Huang, "Fps-net: A convolutional fusion network for large-scale lidar point cloud segmentation," *ISPRS Journal of Photogrammetry and Remote Sensing*, vol. 176, pp. 237–249, 2021.
- [40] Q. Huang, W. Wang, and U. Neumann, "Recurrent slice networks for 3d segmentation of point clouds," in *Proceedings of the IEEE Conference on Computer Vision and Pattern Recognition*, 2018, pp. 2626–2635.
- [41] Y. Zhao, T. Birdal, H. Deng, and F. Tombari, "3d point capsule networks," in *Proceedings of the IEEE/CVF Conference on Computer Vision and Pattern Recognition*, 2019, pp. 1009–1018.
- [42] C. R. Qi, L. Yi, H. Su, and L. J. Guibas, "Pointnet++: Deep hierarchical feature learning on point sets in a metric space," *arXiv preprint arXiv:1706.02413*, 2017.

- [43] H. Zhao, L. Jiang, C.-W. Fu, and J. Jia, "Pointweb: Enhancing local neighborhood features for point cloud processing," in *Proceedings of the IEEE/CVF conference on computer vision and pattern recognition*, 2019, pp. 5565–5573.
- [44] Q. Hu, B. Yang, L. Xie, S. Rosa, Y. Guo, Z. Wang, N. Trigoni, and A. Markham, "Randla-net: Efficient semantic segmentation of large-scale point clouds," in *Proceedings of the IEEE/CVF Conference on Computer Vision and Pattern Recognition*, 2020, pp. 11 108–11 117.
- [45] Y. Wang, Y. Sun, Z. Liu, S. E. Sarma, M. M. Bronstein, and J. M. Solomon, "Dynamic graph cnn for learning on point clouds," *Acm Transactions On Graphics (tog)*, vol. 38, no. 5, pp. 1–12, 2019.
- [46] B. Graham, M. Engelcke, and L. Van Der Maaten, "3d semantic segmentation with submanifold sparse convolutional networks," in *Proceedings of the IEEE conference on computer vision and pattern recognition*, 2018, pp. 9224–9232.
- [47] C. Choy, J. Gwak, and S. Savarese, "4d spatio-temporal convnets: Minkowski convolutional neural networks," in *Proceedings of the IEEE/CVF Conference on Computer Vision and Pattern Recognition*, 2019, pp. 3075–3084.
- [48] S. Xie, J. Gu, D. Guo, C. R. Qi, L. Guibas, and O. Litany, "Point-contrast: Unsupervised pre-training for 3d point cloud understanding," in *European Conference on Computer Vision*. Springer, 2020, pp. 574–591.
- [49] O. Ronneberger, P. Fischer, and T. Brox, "U-net: Convolutional networks for biomedical image segmentation," in *International Conference on Medical image computing and computer-assisted intervention*. Springer, 2015, pp. 234–241.
- [50] Y. Liu, B. Fan, S. Xiang, and C. Pan, "Relation-shape convolutional neural network for point cloud analysis," in *Proceedings of the IEEE/CVF Conference on Computer Vision and Pattern Recognition*, 2019, pp. 8895–8904.
- [51] H. Thomas, C. R. Qi, J.-E. Deschaut, B. Marcotegui, F. Goulette, and L. J. Guibas, "Kpconv: Flexible and deformable convolution for point clouds," in *Proceedings of the IEEE/CVF International Conference on Computer Vision*, 2019, pp. 6411–6420.
- [52] A. Vaswani, N. Shazeer, N. Parmar, J. Uszkoreit, L. Jones, A. N. Gomez, Ł. Kaiser, and I. Polosukhin, "Attention is all you need," *Advances in neural information processing systems*, vol. 30, 2017.
- [53] A. Dosovitskiy, L. Beyer, A. Kolesnikov, D. Weissenborn, X. Zhai, T. Unterthiner, M. Dehghani, M. Minderer, G. Heigold, S. Gelly *et al.*, "An image is worth 16x16 words: Transformers for image recognition at scale," *arXiv preprint arXiv:2010.11929*, 2020.
- [54] Z. Liu, Y. Lin, Y. Cao, H. Hu, Y. Wei, Z. Zhang, S. Lin, and B. Guo, "Swin transformer: Hierarchical vision transformer using shifted windows," in *Proceedings of the IEEE/CVF International Conference on Computer Vision*, 2021, pp. 10 012–10 022.
- [55] H. Zhao, L. Jiang, J. Jia, P. H. Torr, and V. Koltun, "Point transformer," in *Proceedings of the IEEE/CVF International Conference on Computer Vision (ICCV)*, October 2021, pp. 16 259–16 268.
- [56] X. Yu, L. Tang, Y. Rao, T. Huang, J. Zhou, and J. Lu, "Pointbert: Pre-training 3d point cloud transformers with masked point modeling," *arXiv preprint arXiv:2111.14819*, 2021.
- [57] A. Sharma, O. Grau, and M. Fritz, "Vconv-dae: Deep volumetric shape learning without object labels," in *European Conference on Computer Vision*. Springer, 2016, pp. 236–250.
- [58] R. Girdhar, D. F. Fouhey, M. Rodriguez, and A. Gupta, "Learning a predictable and generative vector representation for objects," in *European Conference on Computer Vision*. Springer, 2016, pp. 484–499.
- [59] J. Wu, C. Zhang, T. Xue, W. T. Freeman, and J. B. Tenenbaum, "Learning a probabilistic latent space of object shapes via 3d generative-adversarial modeling," in *Proceedings of the 30th International Conference on Neural Information Processing Systems*, 2016, pp. 82–90.
- [60] J. Xie, Z. Zheng, R. Gao, W. Wang, S.-C. Zhu, and Y. N. Wu, "Learning descriptor networks for 3d shape synthesis and analysis," in *Proceedings of the IEEE conference on computer vision and pattern recognition*, 2018, pp. 8629–8638.
- [61] Y. Yang, C. Feng, Y. Shen, and D. Tian, "Foldingnet: Point cloud auto-encoder via deep grid deformation," in *Proceedings of the IEEE Conference on Computer Vision and Pattern Recognition*, 2018, pp. 206–215.
- [62] J. Li, B. M. Chen, and G. H. Lee, "So-net: Self-organizing network for point cloud analysis," in *Proceedings of the IEEE conference on computer vision and pattern recognition*, 2018, pp. 9397–9406.
- [63] P. Achlioptas, O. Diamanti, I. Mitliagkas, and L. Guibas, "Learning representations and generative models for 3d point clouds," in *International conference on machine learning*. PMLR, 2018, pp. 40–49.
- [64] M. Gadelha, R. Wang, and S. Maji, "Multiresolution tree networks for 3d point cloud processing," in *Proceedings of the European Conference on Computer Vision (ECCV)*, 2018, pp. 103–118.
- [65] Z. Han, M. Shang, Y.-S. Liu, and M. Zwicker, "View inter-prediction gan: Unsupervised representation learning for 3d shapes by learning global shape memories to support local view predictions," in *Proceedings of the AAAI Conference on Artificial Intelligence*, vol. 33, no. 01, 2019, pp. 8376–8384.
- [66] X. Liu, Z. Han, X. Wen, Y.-S. Liu, and M. Zwicker, "L2g auto-encoder: Understanding point clouds by local-to-global reconstruction with hierarchical self-attention," in *Proceedings of the 27th ACM International Conference on Multimedia*, 2019, pp. 989–997.
- [67] Z. Han, X. Wang, Y.-S. Liu, and M. Zwicker, "Multi-angle point cloud-vae: Unsupervised feature learning for 3d point clouds from multiple angles by joint self-reconstruction and half-to-half prediction," in *2019 IEEE/CVF International Conference on Computer Vision (ICCV)*. IEEE, 2019, pp. 10 441–10 450.
- [68] G. Yang, X. Huang, Z. Hao, M.-Y. Liu, S. Belongie, and B. Hariharan, "Pointflow: 3d point cloud generation with continuous normalizing flows," in *Proceedings of the IEEE/CVF International Conference on Computer Vision*, 2019, pp. 4541–4550.
- [69] Y. Shi, M. Xu, S. Yuan, and Y. Fang, "Unsupervised deep shape descriptor with point distribution learning," in *Proceedings of the IEEE/CVF Conference on Computer Vision and Pattern Recognition*, 2020, pp. 9353–9362.
- [70] X. Gao, W. Hu, and G.-J. Qi, "Graphter: Unsupervised learning of graph transformation equivariant representations via auto-encoding node-wise transformations," in *Proceedings of the IEEE/CVF Conference on Computer Vision and Pattern Recognition*, 2020, pp. 7163–7172.
- [71] X. Wen, T. Li, Z. Han, and Y.-S. Liu, "Point cloud completion by skip-attention network with hierarchical folding," in *Proceedings of the IEEE/CVF Conference on Computer Vision and Pattern Recognition*, 2020, pp. 1939–1948.
- [72] Y. Sun, Y. Wang, Z. Liu, J. Siegel, and S. Sarma, "Point-grow: Autoregressively learned point cloud generation with self-attention," in *Proceedings of the IEEE/CVF Winter Conference on Applications of Computer Vision*, 2020, pp. 61–70.
- [73] J. Yang, P. Ahn, D. Kim, H. Lee, and J. Kim, "Progressive seed generation auto-encoder for unsupervised point cloud learning," in *Proceedings of the IEEE/CVF International Conference on Computer Vision*, 2021, pp. 6413–6422.
- [74] M. A. Kramer, "Nonlinear principal component analysis using autoassociative neural networks," *AICHE journal*, vol. 37, no. 2, pp. 233–243, 1991.
- [75] Autoencoder, "Autoencoder — Wikipedia, the free encyclopedia," 2022, [Online; accessed 16-Feb-2022]. [Online]. Available: <https://en.wikipedia.org/wiki/Autoencoder>
- [76] H. Fan, H. Su, and L. J. Guibas, "A point set generation network for 3d object reconstruction from a single image," in *Proceedings of the IEEE conference on computer vision and pattern recognition*, 2017, pp. 605–613.
- [77] S. Sabour, N. Frosst, and G. E. Hinton, "Dynamic routing between capsules," *arXiv preprint arXiv:1710.09829*, 2017.
- [78] S. Chen, C. Duan, Y. Yang, D. Li, C. Feng, and D. Tian, "Deep Unsupervised Learning of 3D Point Clouds via Graph Topology Inference and Filtering," *IEEE Transactions on Image Processing*, vol. 29, pp. 3183–3198, 2020.
- [79] H. Chen, S. Luo, X. Gao, and W. Hu, "Unsupervised learning of geometric sampling invariant representations for 3d point clouds," in *2021 IEEE/CVF International Conference on Computer Vision Workshops (ICCVW)*. IEEE Computer Society, 2021, pp. 893–903.
- [80] I. Goodfellow, J. Pouget-Abadie, M. Mirza, B. Xu, D. Warde-Farley, S. Ozair, A. Courville, and Y. Bengio, "Generative adversarial nets," *Advances in neural information processing systems*, vol. 27, 2014.
- [81] C.-L. Li, M. Zaheer, Y. Zhang, B. Póczos, and R. Salakhutdinov, "Point cloud gan," *arXiv preprint arXiv:1810.05795*, 2018.
- [82] R. Li, X. Li, C.-W. Fu, D. Cohen-Or, and P.-A. Heng, "Pu-gan: a point cloud upsampling adversarial network," in *Proceedings*

- of the IEEE/CVF International Conference on Computer Vision, 2019, pp. 7203–7212.
- [83] E. Remelli, P. Baque, and P. Fua, “Neuralsampler: Euclidean point cloud auto-encoder and sampler,” *arXiv preprint arXiv:1901.09394*, 2019.
- [84] L. Yu, X. Li, C.-W. Fu, D. Cohen-Or, and P.-A. Heng, “Pu-net: Point cloud upsampling network,” in *Proceedings of the IEEE Conference on Computer Vision and Pattern Recognition*, 2018, pp. 2790–2799.
- [85] W. Yifan, S. Wu, H. Huang, D. Cohen-Or, and O. Sorkine-Hornung, “Patch-based progressive 3d point set upsampling,” in *Proceedings of the IEEE/CVF Conference on Computer Vision and Pattern Recognition*, 2019, pp. 5958–5967.
- [86] Y. Qian, J. Hou, S. Kwong, and Y. He, “Pugeo-net: A geometry-centric network for 3d point cloud upsampling,” in *European Conference on Computer Vision*. Springer, 2020, pp. 752–769.
- [87] G. Qian, A. Abualshour, G. Li, A. Thabet, and B. Ghanem, “Pu-gcn: Point cloud upsampling using graph convolutional networks,” in *Proceedings of the IEEE/CVF Conference on Computer Vision and Pattern Recognition*, 2021, pp. 11 683–11 692.
- [88] R. Li, X. Li, P.-A. Heng, and C.-W. Fu, “Point cloud upsampling via disentangled refinement,” in *Proceedings of the IEEE/CVF Conference on Computer Vision and Pattern Recognition*, 2021, pp. 344–353.
- [89] K. Hassani and M. Haley, “Unsupervised multi-task feature learning on point clouds,” in *Proceedings of the IEEE/CVF International Conference on Computer Vision*, 2019, pp. 8160–8171.
- [90] L. Zhang and Z. Zhu, “Unsupervised feature learning for point cloud understanding by contrasting and clustering using graph convolutional neural networks,” in *2019 International Conference on 3D Vision (3DV)*. IEEE, 2019, pp. 395–404.
- [91] Y. Rao, J. Lu, and J. Zhou, “Global-local bidirectional reasoning for unsupervised representation learning of 3d point clouds,” in *Proceedings of the IEEE/CVF Conference on Computer Vision and Pattern Recognition*, 2020, pp. 5376–5385.
- [92] A. Sanghi, “Info3d: Representation learning on 3d objects using mutual information maximization and contrastive learning,” in *European Conference on Computer Vision*. Springer, 2020, pp. 626–642.
- [93] M. Gadelha, A. RoyChowdhury, G. Sharma, E. Kalogerakis, L. Cao, E. Learned-Miller, R. Wang, and S. Maji, “Label-efficient learning on point clouds using approximate convex decompositions,” in *European Conference on Computer Vision*. Springer, 2020, pp. 473–491.
- [94] O. Poursaeed, T. Jiang, H. Qiao, N. Xu, and V. G. Kim, “Self-supervised learning of point clouds via orientation estimation,” in *2020 International Conference on 3D Vision (3DV)*. IEEE, 2020, pp. 1018–1028.
- [95] B. Du, X. Gao, W. Hu, and X. Li, “Self-contrastive learning with hard negative sampling for self-supervised point cloud learning,” in *Proceedings of the 29th ACM International Conference on Multimedia*, 2021, pp. 3133–3142.
- [96] Y. Rao, B. Liu, Y. Wei, J. Lu, C.-J. Hsieh, and J. Zhou, “Randomrooms: Unsupervised pre-training from synthetic shapes and randomized layouts for 3d object detection,” in *Proceedings of the IEEE/CVF International Conference on Computer Vision*, 2021, pp. 3283–3292.
- [97] Z. Zhang, R. Girdhar, A. Joulin, and I. Misra, “Self-supervised pretraining of 3d features on any point-cloud,” in *Proceedings of the IEEE/CVF International Conference on Computer Vision (ICCV)*, October 2021, pp. 10 252–10 263.
- [98] Y. Chen, J. Liu, B. Ni, H. Wang, J. Yang, N. Liu, T. Li, and Q. Tian, “Shape self-correction for unsupervised point cloud understanding,” in *Proceedings of the IEEE/CVF International Conference on Computer Vision*, 2021, pp. 8382–8391.
- [99] T. Groueix, M. Fisher, V. G. Kim, B. C. Russell, and M. Aubry, “A papier-mâché approach to learning 3d surface generation,” in *Proceedings of the IEEE conference on computer vision and pattern recognition*, 2018, pp. 216–224.
- [100] W. Yuan, T. Khot, D. Held, C. Mertz, and M. Hebert, “Pcn: Point completion network,” in *2018 International Conference on 3D Vision (3DV)*. IEEE, 2018, pp. 728–737.
- [101] Z. Huang, Y. Yu, J. Xu, F. Ni, and X. Le, “Pf-net: Point fractal network for 3d point cloud completion,” in *2020 IEEE/CVF Conference on Computer Vision and Pattern Recognition (CVPR)*, 2020, pp. 7659–7667.
- [102] M. Liu, L. Sheng, S. Yang, J. Shao, and S.-M. Hu, “Morphing and sampling network for dense point cloud completion,” in *Proceedings of the AAAI conference on artificial intelligence*, vol. 34, no. 07, 2020, pp. 11 596–11 603.
- [103] W. Zhang, Q. Yan, and C. Xiao, “Detail preserved point cloud completion via separated feature aggregation,” in *Computer Vision—ECCV 2020: 16th European Conference, Glasgow, UK, August 23–28, 2020, Proceedings, Part XXV 16*. Springer, 2020, pp. 512–528.
- [104] C. Xie, C. Wang, B. Zhang, H. Yang, D. Chen, and F. Wen, “Style-based point generator with adversarial rendering for point cloud completion,” in *Proceedings of the IEEE/CVF Conference on Computer Vision and Pattern Recognition*, 2021, pp. 4619–4628.
- [105] Y. Pang, W. Wang, F. E. Tay, W. Liu, Y. Tian, and L. Yuan, “Masked autoencoders for point cloud self-supervised learning,” *arXiv preprint arXiv:2203.06604*, 2022.
- [106] H. Liu, M. Cai, and Y. J. Lee, “Masked discrimination for self-supervised learning on point clouds,” *arXiv preprint arXiv:2203.11183*, 2022.
- [107] K. Fu, P. Gao, S. Liu, R. Zhang, Y. Qiao, and M. Wang, “Posbert: Point cloud one-stage bert pre-training,” *arXiv preprint arXiv:2204.00989*, 2022.
- [108] T. Chen, S. Kornblith, M. Norouzi, and G. Hinton, “A simple framework for contrastive learning of visual representations,” in *International conference on machine learning*. PMLR, 2020, pp. 1597–1607.
- [109] A. v. d. Oord, Y. Li, and O. Vinyals, “Representation learning with contrastive predictive coding,” *arXiv preprint arXiv:1807.03748*, 2018.
- [110] P.-S. Wang, Y.-Q. Yang, Q.-F. Zou, Z. Wu, Y. Liu, and X. Tong, “Unsupervised 3d learning for shape analysis via multiresolution instance discrimination,” *ACM Trans. Graphic*, 2020.
- [111] J. Jiang, X. Lu, W. Ouyang, and M. Wang, “Unsupervised representation learning for 3d point cloud data,” *arXiv preprint arXiv:2110.06632*, 2021.
- [112] J. Hou, S. Xie, B. Graham, A. Dai, and M. Nießner, “Pri3d: Can 3d priors help 2d representation learning?” in *Proceedings of the IEEE/CVF International Conference on Computer Vision (ICCV)*, October 2021, pp. 5693–5702.
- [113] J. A. Hartigan and M. A. Wong, “Algorithm as 136: A k-means clustering algorithm,” *Journal of the royal statistical society. series c (applied statistics)*, vol. 28, no. 1, pp. 100–108, 1979.
- [114] M. Caron, P. Bojanowski, A. Joulin, and M. Douze, “Deep clustering for unsupervised learning of visual features,” in *Proceedings of the European Conference on Computer Vision (ECCV)*, 2018, pp. 132–149.
- [115] J. Sauder and B. Sievers, “Context prediction for unsupervised deep learning on point clouds,” *arXiv preprint arXiv:1901.08396*, vol. 2, no. 4, p. 5, 2019.
- [116] S. Gidaris, P. Singh, and N. Komodakis, “Unsupervised representation learning by predicting image rotations,” in *International Conference on Learning Representations*, 2018.
- [117] A. Thabet, H. Alwassel, and B. Ghanem, “Self-supervised learning of local features in 3d point clouds,” in *Proceedings of the IEEE/CVF Conference on Computer Vision and Pattern Recognition Workshops*, 2020, pp. 938–939.
- [118] C. Sun, Z. Zheng, X. Wang, M. Xu, and Y. Yang, “Point cloud pre-training by mixing and disentangling,” *arXiv preprint arXiv:2109.00452*, 2021.
- [119] J. Behley, M. Garbade, A. Milioti, J. Quenzel, S. Behnke, C. Stachniss, and J. Gall, “Semantickitti: A dataset for semantic scene understanding of lidar sequences,” in *Proceedings of the IEEE/CVF International Conference on Computer Vision*, 2019, pp. 9297–9307.
- [120] A. Xiao, J. Huang, D. Guan, F. Zhan, and S. Lu, “Synlidar: Learning from synthetic lidar sequential point cloud for semantic segmentation,” *arXiv preprint arXiv:2107.05399*, 2021.
- [121] Y. Chen, M. Nießner, and A. Dai, “4dcontrast: Contrastive learning with dynamic correspondences for 3d scene understanding,” *arXiv preprint arXiv:2112.02990*, 2021.
- [122] C. Feichtenhofer, H. Fan, B. Xiong, R. Girshick, and K. He, “A large-scale study on unsupervised spatiotemporal representation learning,” in *Proceedings of the IEEE/CVF Conference on Computer Vision and Pattern Recognition*, 2021, pp. 3299–3309.
- [123] X. Song, S. Zhao, J. Yang, H. Yue, P. Xu, R. Hu, and H. Chai, “Spatio-temporal contrastive domain adaptation for action recognition,” in *Proceedings of the IEEE/CVF Conference on Computer Vision and Pattern Recognition*, 2021, pp. 9787–9795.

- [124] K. Hu, J. Shao, Y. Liu, B. Raj, M. Savvides, and Z. Shen, "Contrast and order representations for video self-supervised learning," in *Proceedings of the IEEE/CVF International Conference on Computer Vision*, 2021, pp. 7939–7949.
- [125] H. Kuang, Y. Zhu, Z. Zhang, X. Li, J. Tighe, S. Schwertfeger, C. Stachniss, and M. Li, "Video contrastive learning with global context," in *Proceedings of the IEEE/CVF International Conference on Computer Vision*, 2021, pp. 3195–3204.
- [126] D. Z. Chen, A. X. Chang, and M. Nießner, "Scanrefer: 3d object localization in rgb-d scans using natural language," in *European Conference on Computer Vision*. Springer, 2020, pp. 202–221.
- [127] M. Kazhdan, T. Funkhouser, and S. Rusinkiewicz, "Rotation invariant spherical harmonic representation of 3 d shape descriptors," in *Symposium on geometry processing*, vol. 6, 2003, pp. 156–164.
- [128] D.-Y. Chen, X.-P. Tian, Y.-T. Shen, and M. Ouhyoung, "On visual similarity based 3d model retrieval," in *Computer graphics forum*, vol. 22, no. 3. Wiley Online Library, 2003, pp. 223–232.
- [129] B. Eckart, W. Yuan, C. Liu, and J. Kautz, "Self-supervised learning on 3d point clouds by learning discrete generative models," in *Proceedings of the IEEE/CVF Conference on Computer Vision and Pattern Recognition*, 2021, pp. 8248–8257.
- [130] M. Afham, I. Dissanayake, D. Dissanayake, A. Dharmasiri, K. Thilakarathna, and R. Rodrigo, "Crosspoint: Self-supervised cross-modal contrastive learning for 3d point cloud understanding," *arXiv preprint arXiv:2203.00680*, 2022.
- [131] H. Deng, T. Birdal, and S. Ilic, "Ppf-foldnet: Unsupervised learning of rotation invariant 3d local descriptors," in *Proceedings of the European Conference on Computer Vision (ECCV)*, 2018, pp. 602–618.
- [132] A. Zeng, S. Song, M. Nießner, M. Fisher, J. Xiao, and T. Funkhouser, "3dmatch: Learning local geometric descriptors from rgb-d reconstructions," in *Proceedings of the IEEE conference on computer vision and pattern recognition*, 2017, pp. 1802–1811.
- [133] Y. Zeng, Y. Qian, Z. Zhu, J. Hou, H. Yuan, and Y. He, "Corrnet3d: unsupervised end-to-end learning of dense correspondence for 3d point clouds," in *Proceedings of the IEEE/CVF Conference on Computer Vision and Pattern Recognition*, 2021, pp. 6052–6061.
- [134] I. Lang, D. Ginzburg, S. Avidan, and D. Raviv, "Dpc: Unsupervised deep point correspondence via cross and self construction," in *2021 International Conference on 3D Vision (3DV)*. IEEE, 2021, pp. 1442–1451.
- [135] H. Jiang, Y. Shen, J. Xie, J. Li, J. Qian, and J. Yang, "Sampling network guided cross-entropy method for unsupervised point cloud registration," in *Proceedings of the IEEE/CVF International Conference on Computer Vision*, 2021, pp. 6128–6137.
- [136] Y. Yan, Y. Mao, and B. Li, "Second: Sparsely embedded convolutional detection," *Sensors*, vol. 18, no. 10, p. 3337, 2018.
- [137] M. Caron, I. Misra, J. Mairal, P. Goyal, P. Bojanowski, and A. Joulin, "Unsupervised learning of visual features by contrasting cluster assignments," *Advances in Neural Information Processing Systems*, vol. 33, pp. 9912–9924, 2020.